TÉCNICO LISBOA

Assessment of Aircraft Icing using Satellite Data

Beatriz Clode Casqueiro

Thesis to obtain the Master of Science Degree in

Aerospace Engineering

Supervisors: Prof. Doutor Pedro Da Graça Tavares Álvares Serrão
Doutora Margarida Belo Pereira

Examination Committee

Chairperson: Prof. Doutor Filipe Szolnoky Ramos Pinto Cunha
Supervisor: Prof. Doutor Pedro Da Graça Tavares Álvares Serrão
Member of the Committee: Doutora Sofia Nunes Lorena Ermida

December 2022

Dedicated to...

My family, who always believed and supported me no matter what.

Acknowledgments

I would like to start my acknowledgments by thanking my supervisors, Professor Pedro Serrão from Instituto Superior Técnico and Dr. Margarida Belo from the Aeronautical Meteorology Division at IPMA (Instituto Português do Mar e da Atmosfera), who were always available to give me the necessary guidance, advice and support. A special thank you to Dr. Margarida Belo for all the help, unthinkable availability and for collecting all the indispensable data.

I would also like to thank Dr. Ricardo Conceição Tavares, Head of the Aeronautical Meteorology Division at IPMA, for his hospitality in letting me use IPMA's facilities and resources. I am also thankful to Dr. Isabel Trigo, for the constructive discussions and for collecting the data of the satellite products.

Last but not least, I would like to extend my deepest gratitude to my family and boyfriend, for always believing, encouraging and motivating me throughout the years.

Resumo

O presente estudo analisa um conjunto de 115 eventos de formação de gelo em aeronaves na Europa Ocidental e Nordeste do Atlântico, utilizando relatos de pilotos (PIREPs) e produtos de satélite. Quatro destes eventos foram analisados com maior detalhe, considerando também a temperatura, a humidade relativa e o conteúdo de água da nuvem (CWC), provenientes de previsões do European Centre for Medium-Range Weather Forecasts. A maioria dos PIREPs de severidade moderada e severa ($> 70\%$) ocorreram nos meses de Outubro a Fevereiro e Outubro a Março, respetivamente. Também foram relatados eventos de formação de gelo na primavera e verão. A maioria dos eventos ocorreu entre FL100 e FL250, com uma percentagem de 82.7% e 78.6%, respetivamente, para a severidade moderada e severa. Os produtos de satélite revelaram que a maioria dos eventos moderados ocorreram em nuvens com um topo composto por gelo, seguido de topos com mistura de fases e água líquida. Quanto aos eventos severos, a maioria esteve associada à presença de gelo e mistura de fases no topo das nuvens, sendo o último o mais frequente. A maioria das ocorrências esteve associada a nuvens média/altas, com temperaturas de brilho de $10.8\mu m$ (BT10.8) entre os $-40°C$ e os $-8°C$. Por último, os quatro casos analisados revelaram valores baixos de CWC ($< 0.18g/kg$) e valores elevados de humidade relativa ($> 74.8\%$). Ademais, em dois eventos o fenómeno de formação de gelo ocorreu abaixo do topo da nuvem e nos outros dois perto do topo (com uma temperatura próxima da BT10.8).

Palavras-chave: formação de gelo nas aeronaves, PIREP, produtos de satélite, modelo do ECMWF, conteúdo em água líquida

Abstract

A sample of 115 aircraft icing events in the Western Europe and Northeastern Atlantic sector is studied, using pilot reports (PIREPs) and satellite observations and products. A detailed study of four events is performed, using also temperature, relative humidity and cloud water content (CWC) provided by the European Centre for Medium-Range Weather Forecasts model. Most of the moderate and severe icing PIREPs ($> 70\%$) occurred between the months of October and February, and October and March, respectively. Icing events were also reported during final spring and summer months. Most of the events occurred between flight level (FL) FL100 and FL250, with a percentage of 82.7% and 78.6%, respectively, for moderate and severe icing. Moreover, the satellite products revealed that a great amount of the moderate icing events occurred in a cloud-filled environment with ice cloud-top phase, followed by mixed and water. For severe icing events, the majority of the cases were associated with ice and mixed cloud-top phases, the latter being the most frequent. Most of the icing events were associated with medium and high opaque clouds and $10.8\mu m$ brightness temperatures (BT10.8) between $-40°C$ and $-8°C$. Lastly, the four cases analyzed were associated with small values of CWC ($< 0.18 g/kg$) and high values of relative humidity ($> 74.8\%$). Moreover, in two events, aircraft icing happened below the cloud-top and two other occurred near the cloud-top (with a temperature close to the BT10.8).

Keywords: aircraft icing, PIREP, satellite products, ECMWF model, liquid water content

Contents

List of Tables

List of Figures

Acronyms

AIRMETs Airman's Meteorological Information

AWAD Aviation Weather Accidents Database

BT Brightness Temperature

BT10.8 10.8μm Brightness Temperature

CWC Cloud Water Content

DivMA Aeronautical Meteorology Division

ECMWF European Centre for Medium-Range Weather Forecasts

EUMETSAT European Organization for the Exploitation of Meteorological Satellites

FIRs Flight Information Regions

FL Flight Level

IPMA Instituto Português do Mar e da Atmosfera

LWC Liquid Water Content

MED Mean Effective droplet Diameter

MSG Meteosat Second Generation

MWO Meteorological Watch Office

NWP Numerical Weather Prediction

OPMET Operational Meteorological

PIREPs Pilot Reports

RH Relative Humidity

SEVIRI Spinning Enhanced Visible and InfraRed Imager

SIGMETs Significant Meteorological Information

T Temperature

T2m Two-meter temperature

WMO Weather Meteorological Organization

Chapter 1

Introduction

The purpose of this first chapter is to introduce the phenomenon of aircraft icing and, given its unquestionable impact on flight safety, justify the motivation for its study. Furthermore, the ongoing section will describe the thesis objectives and deliverables, and briefly explain the contents of the different chapters.

1.1 Motivation

Since the earliest days of aviation industry, weather has been recognized to have a major impact on air transport safety. Due to the progress made in technology throughout the years, airborne, satellite and instrument landing systems have evolved, and together with Numerical Weather Prediction (NWP) forecasts [1, 2], the absolute number of casualties due to aircraft disasters has decreased notably. Regardless of the improvements made, according to the Aviation Weather Accidents Database (AWAD), the percentage of casualties in accidents due to the weather shows a modest increase between 1967 and 2010 [3]. Also, meteorological conditions are still one of the most significant causes of incidents and accidents in aviation [3].

Aircraft icing may occur throughout flights in the presence of supercooled liquid water clouds or mixed-phase clouds [4]. Icing is one of the meteorological phenomena that contributes for air transport accidents associated with weather conditions. Aircraft icing is of significant concern for aviation safety to the extent that, between 1998 and 2009, not less than 565 aircraft accidents were associated to ice accretion, in both commercial and non-commercial airplanes, in the United States [5]. Worldwide, aircraft icing is accountable for approximately 7%, 10% and 9% of the meteorological-caused accidents in the climb, approach and landing phases, respectively [3].

To better understand the severity of this threat, wind tunnel and flight tests made by the Air Safety Foundation AOPA [6] have shown that icing accretions on the wing can lead to a decrease of 30% in lift and an increase up to 40% in drag. Furthermore, a NASA study demonstrated that almost 30% of the total drag derived from an icing event persisted even after the protected areas were cleared [6].

To prevent icing disasters, the airplane system can be designed and developed with icing tolerant

characteristics, or the aircraft route can avoid icing prone areas. Although the latter would heavily increase aviation safety, this task is more difficult to perform in commercial aircraft, due to schedules constraints. Therefore, ice tolerance is an essential attribute of the airplane [7]. It is important to note that the influence of in-flight icing will vary with the type of aircraft. Jet aircraft are usually less vulnerable to icing because of their bigger propulsion power, which allows them to perform escaping maneuvers much more easily. Whereas medium and small sized aircraft are more vulnerable to icing because they generally operate at medium flight levels where the icing potential is higher, making them to completely depend on their deicing and anti-icing equipment [8].

As such, it is obvious that aircraft icing endures as a serious risk to aviation. Therefore, monitoring and forecasting the icing phenomenon, areas of risk and its severity, is a major challenge to meteorologists and is of undeniable relevance [9]. This is why conducting a detailed study about aircraft icing is of the utmost importance.

Note that a significant part of the accidents due to the weather occurs in latitudes between 12° and 38° in both north and south hemispheres [3], which includes part of the Portuguese Flight Information Regions (FIRs): Lisbon and Santa Maria Oceanic. This is of significant importance, since the Aeronautical Meteorology Division (DivMA) at the Portuguese Institute for Sea and Atmosphere (IPMA) as a Meteorological Watch Office (MWO), is responsible for maintaining constant watch and providing the necessary information for the safety, regularity and efficiency of air navigation for the two Portuguese FIRs [10]. Moreover, DivMA is also responsible for regularly providing meteorological information when severe - Significant Meteorological Information (SIGMETs) - or moderate - Airman's Meteorological Information (AIRMETs) - aircraft icing events have occurred, or are expected to occur [11].

1.2 Objectives and Deliverables

Over the years, several studies were devoted to aircraft icing over North America [7, 12–17], however, over the western Europe only few studies addressed this topic [9, 18]. The current study aims to characterize the aircraft icing environment in Western Europe and Northeastern Atlantic sector, using pilot reports (PIREPs) and satellite observations. A sample of 115 PIREPs is considered, where 86 of the reports are of moderate icing and 29 are of severe icing. The analyzed cases took place between January 2019 and March 2022. Besides, a more detailed analysis of four events is performed, using also forecasts of temperature, relative humidity and cloud water content provided by the European Centre for Medium-Range Weather Forecasts (ECMWF) model. These data are important to improve icing algorithms based on NWP forecasts, such as that currently used operationally at the Portuguese MWO [9]. As a result of this study, an article was written and submitted to Atmospheric Research journal in Elsevier (Casqueiro et al. [19]).

1.3 Thesis Outline

This thesis consists of five chapters. The second chapter presents a succinct description of aircraft icing and the related phenomena in order to provide the foundations utilized to characterize this meteorological event, like the atmospheric conditions that lead to its formation and the aircraft characteristics that impact the occurrence of icing. The third chapter will focus on the data involved in the current work, such as the pilot reports' database, the satellite observations and the forecast data, and the methodology applied. The fourth chapter provides results from the PIREPs, satellite products and ECMWF model. A statistical analysis of the overall view and a few cases studies are presented. At last, the fifth chapter will recapitulate the main conclusions of the thesis and provide some suggestions for future research.

Chapter 2

Background

This chapter begins by describing the aircraft icing phenomenon. A description of the classification system of icing severity and its different physical types is presented. A characterization of the atmospheric conditions that lead to its formation and aircraft features that impact the occurrence of icing then follows. Lastly, notable aircraft icing effects and icing detection are briefly described.

2.1 Theoretical Overview

At temperatures below $-36°C$ to $-40°C$, liquid water droplets freeze spontaneously through homogeneous nucleation, depending on the diameter droplet [20]. In contrast, at sub-freezing temperatures above these values, the freezing of liquid water droplets usually requires the presence of ice nuclei [21, 22]. However, the availability of ice nuclei in the atmosphere is small, especially at temperatures above $-10°C$ [23]. Therefore, liquid droplets at sub-freezing temperatures, known as supercooled water droplets, have been observed in several types of clouds [20, 24–26]. In-flight icing is defined as the accretion of ice on the airframe during flight, caused by the presence of supercooled water droplets [27]. These droplets are unstable and once hitting a cold object, they can freeze and form a thin coat of ice. This is the elementary mechanism for the icing phenomenon [27, 28].

2.1.1 Icing Severity

Although there are three types of aircraft icing - structural, instrument and induction -, weather forecasters are only concerned with structural icing, which corresponds to the ice accretion on the exterior surfaces of the airframe [29]. It is important to note that there are several factors that influence the rate of ice accumulation in structural icing, which can make it difficult to correctly identify the icing threat to any particular airplane [29]. Therefore, it is important to classify the icing phenomenon into severity categories, which describe the impact of accreted ice on the flight of an aircraft [9]. Over the years, icing severity has been a matter of debate. In the $50s$ and $60s$, icing severity has been classified into five or four classes [30], as illustrated in the tables depicted in Figures 2.1 and 2.2.

Descriptive terminology	Aircraft performance criteria	Liquid water content (g/m^3)	Ice collection rates on small probes	
			Inches per 10 miles	Miles per 1/2 inch
Trace	Barely perceptible formations on unheated aircraft components	0 to 0.125	0 to 0.09	56 or more
Light	Evasive action unnecessary (no perceptible effects on performance)	0.125 to 0.25	0.09 to 0.18	28 to 56
Moderate	Evasive action desirable (noticeable effects on performance)	0.25 to 0.60	0.18 to 0.36	14 to 28
Heavy	Eventual, evasive action necessary (aircraft is unable to cope with icing situation and extended operation is not possible)	0.60 to 1.0	0.36 to 0.72	7 to 14
Severe	Immediate evasive action is required (aircraft uses climb power to hold altitude, and continued operation is limited to a few minutes)	1.0 or more	0.72 or more	0 to 7

Figure 2.1: 1956 US Air Force standards of aircraft icing severity [30].

Icing severity level	Light	Moderate	Heavy	Severe
Icing intensity	<0.6	0.6–1.0	1.1–2.0	>2.0

Figure 2.2: Icing severity level [30].

Today, according to the Weather Meteorological Organization (WMO) the severity of aircraft icing [31] is classified as:

- light - Accumulation rate may create a problem if flight in this environment exceeds 1 hour;
- moderate - Rate of accumulation is such that even short encounters are potentially hazardous. Anti-icing equipment must be used;
- severe - Rate of accumulation is such that use of anti-icing equipment fails to reduce or control the hazard. Immediate diversion from the region is necessary.

While the first level does not represent a problem, the last two categories pose a threat to flight safety [12, 27, 30]. Although in North America the icing severity is reported for 8 different icing categories, including no icing [32], in Europe only moderate and severe icing events are usually reported, since this is mandatory according to the International Civil Aviation Organization (ICAO) [11]. As such, only these two categories will be analyzed here.

2.1.2 Types of Icing

Normally, aircraft icing can be divided into three physical types: rime, glaze and mixed ice, the latest being a combination of the first two types [17, 23, 27, 30]. Rime ice may be formed when tiny, supercooled liquid droplets collide on the wing of the airplane and freeze instantly, before having time to spread away [23]. Although this type of ice can redistribute the stream of air over the wing in a greater way than glaze ice can, it has a lower weight and is easier to remove with deicing equipment [23]. Glaze ice, also known as clear ice, can be formed when the aircraft flies through an area of large supercooled droplets [17]. Upon impact on the airplane, the drops break apart and flow along the airframe before freezing into a smooth and transparent ice [27]. Therefore, clear ice can possibly flow to unprotected areas and accrete there [27], hampering the removal of icing. Hence, glaze ice has a greater impact on the performance of the aircraft when compared to rime and mixed ice [30, 33], as confirmed by the results from five icing research flights by Mikkelson [34].

2.1.3 Atmospheric Variables and Type of Clouds that contribute to the occurrence of Icing

In general, aircraft icing occurs in extensive layers of clouds, where considerable amounts of liquid water are available and the temperature is below freezing. Moreover, the severity of aircraft icing depends on three atmospheric parameters: the liquid water content (LWC), the mean effective droplet diameter (MED) and the ambient temperature [35–37]. Since water in the liquid state tends to exist in larger concentrations in warmer air and diminishes with decreasing temperature, icing generally occurs at temperatures between $-40°C$ and $0°C$, being more frequent between $-20°C$ and $0°C$ [27, 28, 38, 39]. Moreover, severe icing takes place normally between $-15°C$ and $0°C$ [30, 35]. Therefore, aircraft icing conditions tend to form below 8000 meters (26000 feet) [27, 33, 40]. The altitude at which aircraft icing occurs varies with the latitude: Politovich et al. [27] showed that at lower latitudes in the Northern Hemisphere (e.g., around $15°N$) the favorable temperatures for icing in January take place between flight level (FL) FL160 and FL260, and at higher latitudes (like $70°N$) below FL045. For mid-north latitudes like $45°N$, the favorable temperatures for icing take place below FL160 [27]. In essence, lower latitudes in the Northern Hemisphere are associated with warmer temperatures, so the altitudes conducive to icing are higher, and higher latitudes are associated with colder temperatures, so the altitudes conducive to icing are lower.

The first parameter, LWC, which is liquid water per unit volume, is one of the most crucial variables with impact on aircraft icing. The greater the LWC, the more significant is the icing risk [30]. In convective clouds the LWC is generally $< 0.5 - 0.7\,g/m^3$ ($\sim < 0.366 - 0.511\,g/kg$), and in stratiform clouds $< 0.3 - 0.5\,g/m^3$ ($\sim < 0.219 - 0.366\,g/kg$) [27]. More specifically, Curry et al. [41] showed that, in the mid-latitude regions of the North Atlantic Ocean, the average value of the cloud's LWC was approximately $0.095\,g/m^3$ ($\sim 0.069\,g/kg$) for low-level clouds and $0.043\,g/m^3$ ($\sim 0.031\,g/kg$) for mid-level clouds (the definition of low, mid and high-level clouds is presented at the end of this section). Also, maximum values of cloud's LWC were $0.63\,g/m^3$ and $0.40\,g/m^3$ ($\sim 0.46\,g/kg$ and $0.29\,g/kg$, sequentially) for low and mid-level supercooled clouds, respectively. For the unit conversion, the air density at $-15°C$ was used.

Finally, the greater the MED, the higher is the impact on the airplane since the thickness of the ice increases [30]. Furthermore, for a water droplet's diameter between $15\,\mu m$ and $40\,\mu m$, the larger the MED, the greater the inertia, which complicates the deviation of the water droplets from the initial trajectory, and increases the chance of the wing leading edge to be iced. For diameters below $15\,\mu m$, the droplets will stay in the free-stream and will not interfere with the surfaces of the airplane, contributing less for ice accretion [30, 40]. The most dangerous icing events occurred in situations where supercooled droplets of $40 - 300\,\mu m$ diameter were present [33]. Note that the icing severity depends on the relationship between LWC and MED [37, 39, 42], so that larger MED requires smaller LWC values and vice versa. LWC greater than $0.2 g/m^3$ and MED greater than $30\,\mu m$ represent the conditions impacting most heavily on aircraft performance [35, 37]. Moreover, the presence of large droplets is normally associated to fairly warm cloud-top temperatures ($> -15°C$) and low LWC [43, 44]

The risk of this phenomenon increases with large concentrations of supercooled liquid water and/or with the presence of large droplets [35]. Aircraft icing can be caused by cumuliform and stratiform clouds [33]. Cumuliform clouds have a considerable vertical extent, are unstable and more energetic than stratiform clouds and therefore, usually produce higher LWCs and MEDs [30], which increases its impact on icing formation. Conversely, stratiform clouds have a smaller vertical depth but a larger horizontal extent, and in general, a lower LWC and water droplet diameter [30, 40]. Nevertheless, Marwitz et al. [42] showed that in situations of temperature inversion, stratiform clouds could also contain large droplets. In single cloud layers, water drop diameter and LWC normally increase with height, which makes the cloud top the most notable icing potential region [27]. The type of cloud also influences the duration of the aircraft icing. Bearing in mind that the impact of this phenomenon cannot be neglected during the climb and descent phases in commercial aircraft [3] and cumuliform clouds have a larger vertical extent, the airplane will remain for a longer period of time inside the cloud which will increase the duration of the aircraft icing event.

Clouds are generally classified into four main groups taking into account the height of the cloud's base above the surface, namely: low-level clouds, mid-level clouds and high-level clouds, and clouds with vertical development [45]. Low clouds are generally composed of water droplets, being able to also contain ice particles in cold weather. Middle Clouds are mainly composed of water droplets and some ice crystals, when the temperature gets sufficiently low. For higher altitudes, the air is extremely cold and dry which explains the composition of high clouds, almost uniquely ice crystals. Finally, clouds with vertical development generally have a lower and warmer region composed of water droplets, a higher and colder part composed only of ice crystals, and a mixed phase in between. Note that clouds cannot be precisely identified only based on elevation, since the corresponding altitude of each group overlaps and varies with latitude (see Table 2.1).

Table 2.1: Approximate Height of Cloud Bases for Different Latitudes [45].

Cloud Group	Tropical Region	Middle Latitude Region	Polar Region
High	6-18 km (19685 - 59055 ft)	5-13 km (16400 - 42650 ft)	3-8 km (9840 - 26240 ft)
Middle	2-8 km (6560 - 26240 ft)	2-7 km (6560 - 22970 ft)	2-4 km (6560 - 13120 ft)
Low	0-2 km (0 - 6560 ft)	0-2 km (0 - 6560 ft)	0-2 km (0 - 6560 ft)

2.1.4 Aircraft Characteristics that impact the occurrence of Icing

There is a vast number of aircraft characteristics that may impact differently the occurrence of icing, such as the speed of the aircraft, the aircraft size and the type of deicing and/or anti-icing equipment employed [28].

The aircraft speed may impact the ice accretion through kinetic heating [28]. The greater the speed, the larger the kinetic heating, which consequently increases the temperature, decreasing the accumulation of ice and the risk of aircraft icing. For example, for a velocity around $460 km/h$ $(250 kt)$, the kinetic heating is fairly $+10°C$. This increment of temperature takes place at the leading edge of the airplane,

shielding it from the icing phenomenon, considering that the air temperature is above $-10°C$ [28]. For a true airspeed greater than $981 km/h$ $(530 kt)$, at sea level, or $1074 km/h$ $(580 kt)$, at $6096 m$ $(20000 ft)$, the kinetic heat can melt the ice entirely. Hence, it is possible to eliminate the anti-icing equipment, according to the US military standard (MIL-A9482) [30, 46].

In general, smaller aircraft fly at lower altitudes where icing conditions are more frequent which, along with their diminished reserve power and de-icing capabilities, makes them more vulnerable to aircraft icing. On the other hand, for larger aircraft cruising at altitudes above icing-prone layers, icing conditions are only found during the ascent and descent maneuvers [27].

Moreover, depending on the location of the aircraft where the icing phenomenon forms, different effects may occur. One of the main characteristics that airframes must be designed with is smooth areas to facilitate the airflow, so that the greatest lift force can be produced. When ice is formed on the wings or fuselage, the airflow may be disturbed and turbulence may be established, increasing the drag (which increases with the exposure time to the icing event) and decreasing the lift capability of the airplane, as shown by the performance data on a wing, acquired by Nasa Glenn Research Center at Lewis Field (Figure 2.3). At some airports, a layer of frost may be formed during night time, contributing to a more turbulent and thicker boundary layer, and decreasing the angle of attack at which flow separation occurs [27, 28]. Additionally, when formed at the intake of the engine, the ice decreases the power of the aircraft, since it diminishes the available oxygen to burn [23, 30].

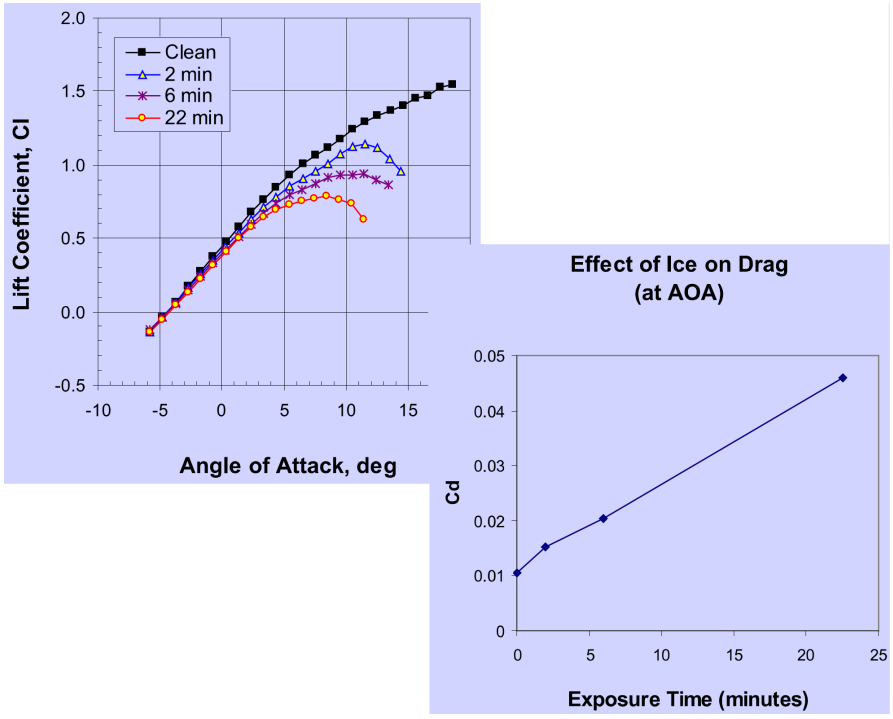

Figure 2.3: Icing effects on aircraft performance variables: lift, angle of attack and drag [47].

2.1.5 Icing Effects and Icing Detection

The icing phenomenon can affect the performance of an airplane in multiple ways. While it decreases lift and the rate of climb, it increases drag since it disturbs the smooth flow of air [6, 18]. Consequently, the aircraft may stall at lower angles of attack and higher velocities [6]. To counterbalance the additional drag, power is added to the engines, which increases fuel consumption [30]. The total weight of the airplane increases due to the additional weight of the ice accumulated, but in an insignificant way when compared to the airflow disruption caused. Besides these main effects, icing can also obstruct the engine's air intake in a fuel-injected engine and ice up the carburetor, which may cause engine stoppage [6, 18].

It is then possible to conclude that the icing phenomenon has numerous effects on an aircraft: decrease of lift and stall angle of attack, increase of drag and critical stall speed, decline of performance due to iced air intake on the engines, and reduction of control efficiency [30, 47].

Generally, pilots have a defective view of the airplane's wings so they normally use the ice accreting on wipers, windshields, and/or pitot tubes near the nose of the aircraft to evaluate the presence and quantity of ice [27]. There are also onboard icing detectors that alert the pilot when ice is accumulating on the airplane, which may provide a premature warning of ice accreting to the pilot. The benefit of in situ instruments is that they give a positive detection of aircraft icing conditions. Nonetheless, they have the downside that the airplane must be immersed in the icing environment which is not a preferable place to be [27].

Chapter 3

Data and Methodology

This third chapter is mostly dedicated to the description of the data and methodology used in the current work. Three types of data will be used to study the icing phenomenon. The pilot reports' database is described, from the information included in the reports to the time range considered. Satellite observations and products are also taken into account, and the forecast data is described. Finally, a brief explanation of the methodology applied is presented.

3.1 Pilot Reports

As expected, PIREPs are more recurrent during the day and more often find near significant airports and flight routes with hefty traffic [9]. Additionally, the reported severity of the icing event is determined by the pilot and will vary with the type of airplane, so different aircraft will observe and report different icing intensities in the same icing environment [48]. Consequently, PIREPs tend to be subjective and dependent on the pilot and the airplane. Furthermore, reports of 'no icing' may not happen since pilots are not required to do so [12], delays may occur in providing the icing report that will lead to a notable error in time and location [49], and areas of deep convection which are typical of cumuliform clouds and are often associated with icing events are normally avoided. Hence, the PIREPs are sporadic, non-systematic and their distribution is biased [50]. Due to these limitations, PIREPs are not suitable to perform a climatology of the aircraft icing. Nonetheless, this type of data is very useful in providing icing information and verifying icing forecasts.

This work uses a sample of 115 PIREPs provided by IPMA through the Regional OPMET (Operational Meteorological) Centres of Toulouse (for the region of Spain) and London (for the regions of Ireland, Wales and England) and IPMA itself (for the Santa Maria and Lisbon FIRs) [51]. From the reports, 86 are of moderate intensity and 29 are of severe intensity. Each report contains information on severity, date, time, latitude, longitude and flight level. A flight level is the height, expressed in hundreds of feet, above the standard mean sea level pressure of 1013.25hPa at which that pressure occurs in the ICAO standard atmosphere [11].

The location of the icing reports includes the western Europe and Northeastern Atlantic sector and

is shown in Figure 3.1. The analyzed cases were reported between January 2019 and March 2022.

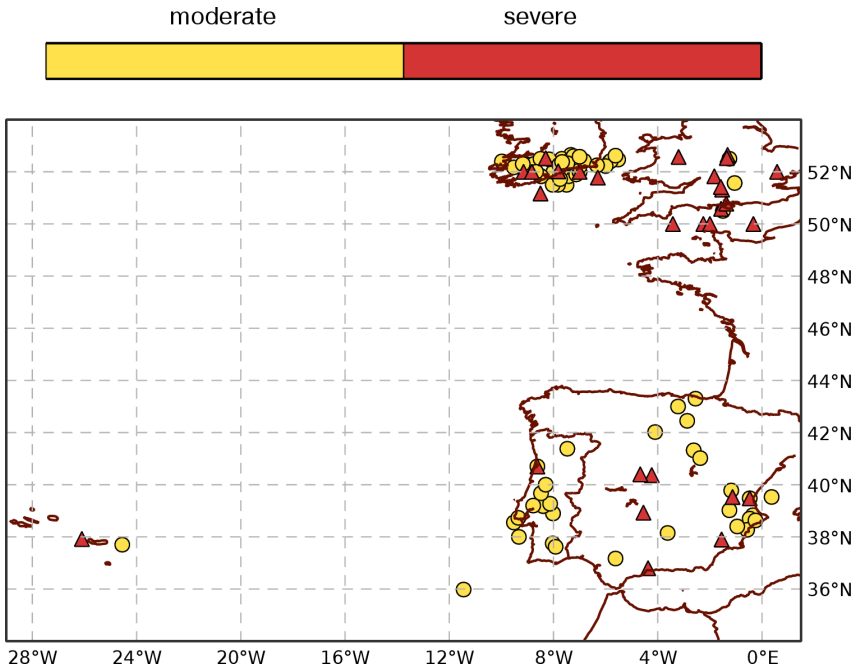

Figure 3.1: Location of icing pilot reports.

Regarding the PIREPs spatial distribution, it is evident that there were more icing occurrences north to the $45°N$ parallel than south, 72 and 43 cases, respectively (see Figure 3.2). This would be expected as the region north to $45°N$ generally comprises lower temperatures associated to icing events. Most of the reports collected north (south) of $45°N$, approximately 70% of the events, occurred in October and between the months of December and March (most of them occurred between October and January for the reports collected south of $45°N$).

Concerning the selected PIREPs, the most frequent reports were of moderate icing. This would be expected since more extreme icing conditions are normally avoided, such as cumulonimbus or thunderstorm clouds (cumuliform type of cloud) which interfere with aircraft flights in various ways. Most of the moderate and severe icing reports ($> 70\%$) occurred between the months of October and February, and October and March, respectively (see Figure 3.3). Even though at first sight aircraft icing would be expected more frequently during the cold months of the year (since the meteorological conditions associated to icing are more common during wintertime), as shown in the previous graph, icing events were also reported during final spring and summer months, which is coherent with previous studies like in Sand et al. [33] and Politovich [44]. Approximately 10% of moderate events were reported between July and August and 14% of severe events between May and June. The seasonal and inter-annual atmospheric variability explains this.

Once again, regarding the reports' spatial distribution, it is evident that most of the events north and south of $45°N$ occurred between FL100 and FL250 and between FL150 and FL≥ 250, respectively (see Figure 3.5), which is consistent with the altitude range at which aircraft icing was found in other studies like in Politovich et al. [27] and Sand et al. [33]. It should be noted that north of $45°N$ there were more icing events between FL100 and FL150 (20.6%) than above FL250 (2.9%), while south of $45°N$ there were

more icing events above FL250 (16.7%) than between FL100 and FL150 (11.9%). This would be expected as the region north of $45°N$ generally gets lower temperatures at inferior altitudes than the region south of $45°N$. Note that the lapse rate, the rate at which the temperature decreases with altitude, is normally 6 to 7 degrees per km [52]. Hence, it will be assumed a lapse rate of $6.5°C/km$ and that, for example, in December, the average temperature in Lisbon, a region south of $45°N$, is $11°C$, while in London, a region north of $45°N$, is $5.6°C$ [53]. Therefore, it is possible to infer that the majority of the icing events north of $45°N$, accordingly with the average temperature in London, occurred between the temperatures of $-14°C$ (FL100) and $-44°C$ (FL250), while south of $45°N$, accordingly with the average temperature of Lisbon, occurred between the temperatures of $-18°C$ (FL150) and $-38°C$ (FL250).

Regarding to Figure 3.5, most of the events occurred between FL100 and FL250, with a percentage of 82.7% and 78.6% for the moderate and severe events, respectively. In contrast, about 7% and 10% of the moderate events took place below FL100 and above FL250, while 18% and 3.5% of the severe events occurred below FL100 and above FL250.

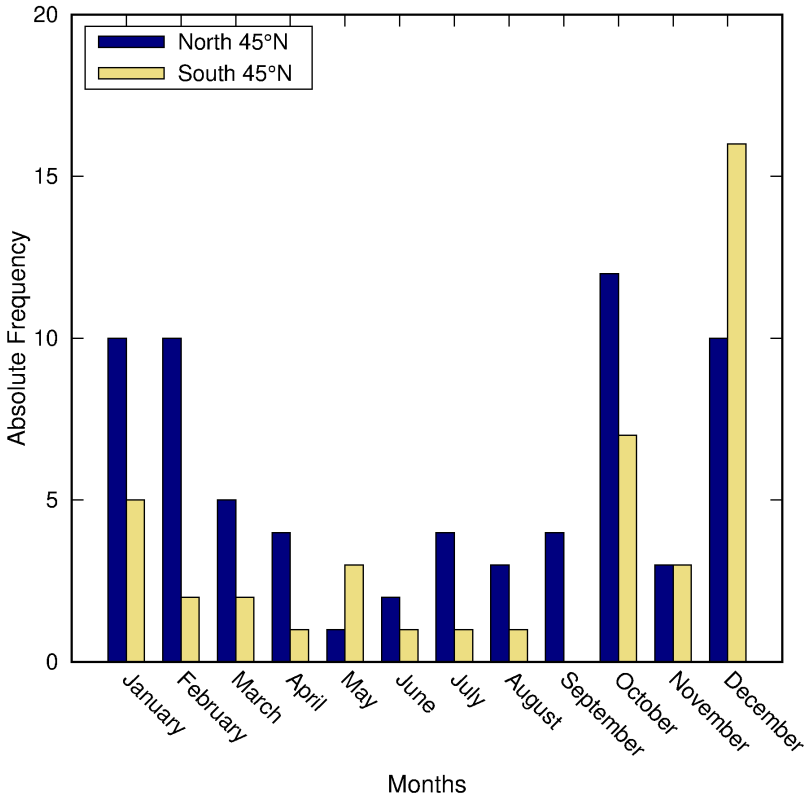

Figure 3.2: Distribution of icing PIREPs located north and south of the $45°N$ parallel respectively, by months.

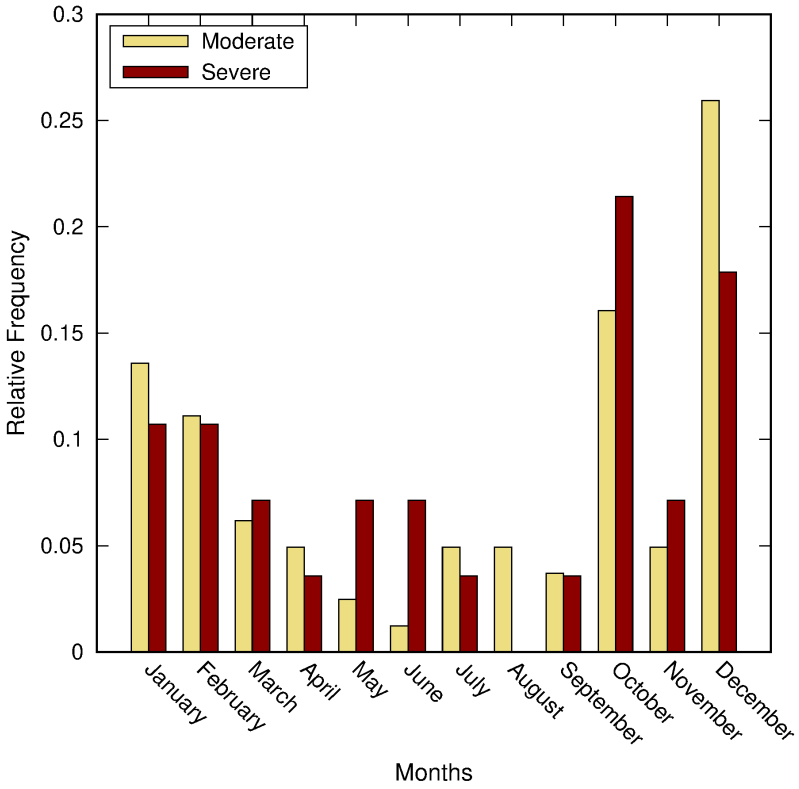

Figure 3.3: Distribution of moderate and severe icing PIREPs by months.

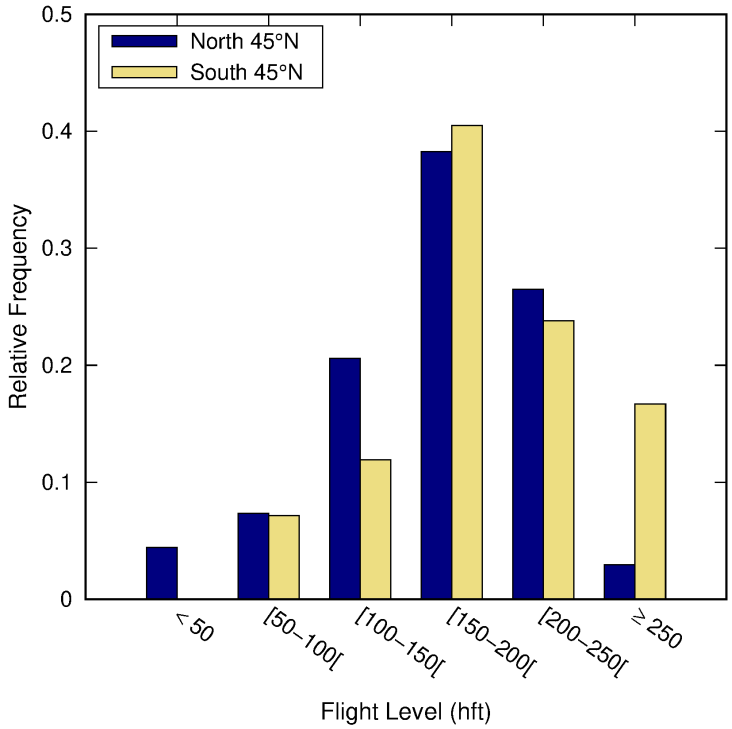

Figure 3.4: Distribution of icing PIREPs located north and south of $45° N$ parallel respectively, by altitude (flight level).

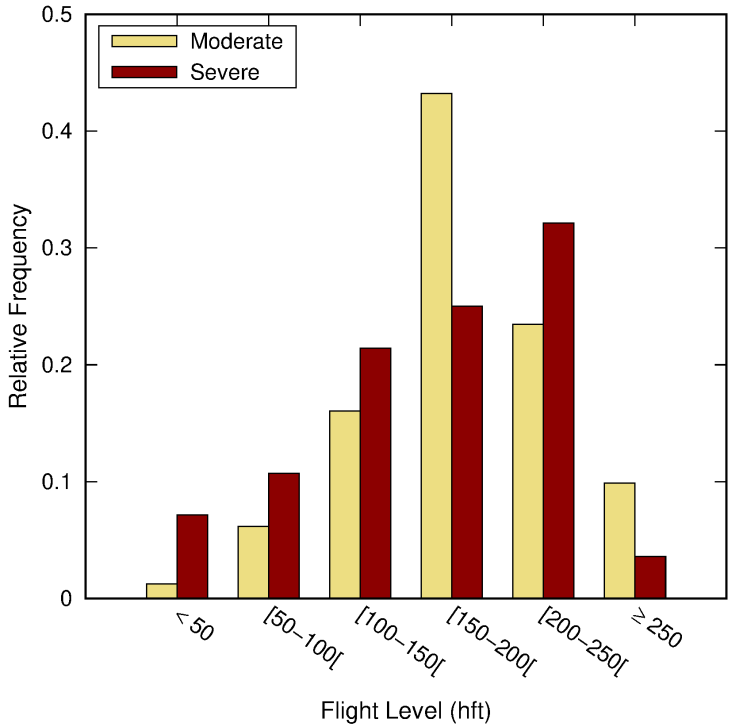

Figure 3.5: Distribution of moderate and severe icing PIREPs by altitude (flight level).

3.2 Satellite Observations

Aircraft icing conditions occur in regions where the top cloud temperature is below freezing, cloud depth is larger than $1000m$ and where significant amounts of liquid water exist [41]. Thus, although the icing phenomenon cannot be directly observed from satellite data, some satellite products provide information about cloud properties that may help identifying areas which favor icing conditions [38, 41]. There are two types of weather satellites: Polar-orbiting, which orbit nearly parallel to the earth's meridian lines, and Geostationary (or geosynchronous), which can observe a fixed area (or disc) of the earth, since they orbit the equator at the same earth's rotation rate [45].

In this study, the satellite data was obtained through the geostationary Meteosat Second Generation (MSG) satellite from the European Organization for the Exploitation of Meteorological Satellites (EUMETSAT). The Meteosat satellite provides full disc imagery every fifteen minutes over Europe and Africa [54]. MSG satellites carry on board a primary instrument, the Spinning Enhanced Visible and InfraRed Imager (SEVIRI), that has the ability to observe the Earth atmosphere using 12 different spectral channels. Eight of these are thermal infrared channels (3.9, 6.2, 7.3, 8.7, 9.7, 10.8, 12.0 and $13.4\mu m$), which provide information both day and night [55]. The remnants are three channels in the solar spectrum (0.6, 0.8 and $1.6\mu m$) and a broadband high-resolution visible channel, which are available only during daytime. The high-resolution visible channel has a spatial resolution at the sub-satellite point of $1km$, while the other have a spatial resolution of $3km$ [55].

The satellite data and products employed in this study include brightness temperature (BT) for the

channel centred at $10.8\mu m$, cloud mask, cloud-top phase and cloud type. The $10.8\mu m$ brightness temperature, a channel in the thermal infrared window, gives a good estimate of the cloud top temperature, although the exact value depends on cloud characteristics [56]. The cloud mask product identifies cloudy and cloud free areas, flagging also the presence of snow/sea ice on the ground [57]. An example of a cloud mask product used in this work is shown in Figure 3.6. The cloud-top phase product allows identifying cloud tops composed of water, ice or both (mixed) (example shown in Figure 3.7). The cloud type product (see example in Figure 3.8) classifies clouds into several classes: high, medium, low and very low clouds (including fog), fractional clouds and semitransparent clouds [57]. These products rely on the fact that, on a given spectral range, brightness temperatures and reflectance of clouds depend on their characteristics, such as height (low, medium or high-level clouds), amount (semi-transparent or opaque) or phase (water or ice clouds), among others. For instance, the visible channels are useful to distinguish thick clouds, which have a higher albedo (reflectivity) from thin clouds. The brightness temperature difference (BT$10.8\mu m$ - BT$12.0\mu m$) is usually higher for cirrus clouds than for thick clouds. Cloud free areas covered by snow or ice are identified at daytime with their very low reflectivity at $1.6\mu m$ or $3.8\mu m$ and high reflectivity at $0.6\mu m$, whereas oceanic cloud free areas affected by sun glint are identified by their very high reflectivity at $3.8\mu m$. Water clouds usually have a low difference BT$8.7\mu m$ - BT$10.8\mu m$ and ice clouds rather high values. This knowledge together with other information is used to estimate the cloud phase of the cloud top. Note that satellite observations allow the classification of the cloud phase at the highest levels of identified clouds, consequently, the presence of liquid water at lower altitudes within the cloud may be under-detected. It is also important to mention that warm objects radiate more energy than cold bodies. Thus, since the top of low clouds are warmer than high clouds, infrared channels can distinguish warm low clouds (higher BT) from cold high clouds (lower BT) [45].

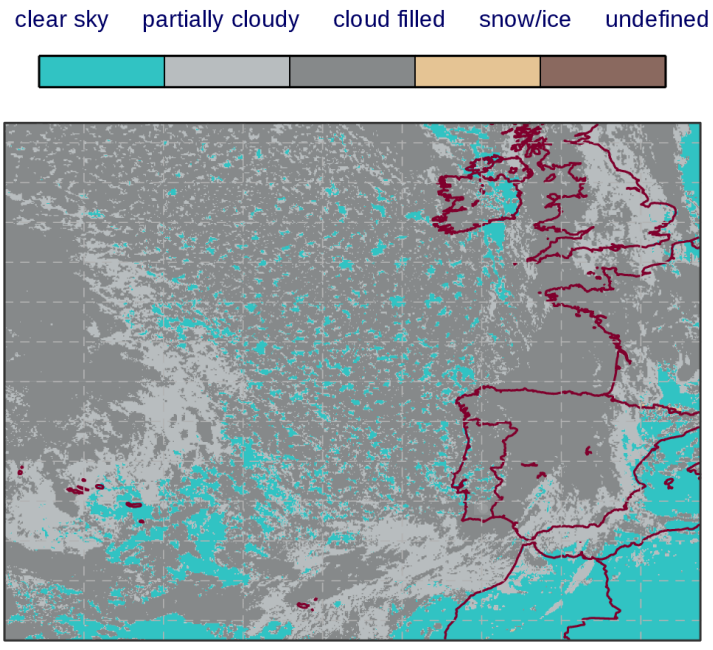

Figure 3.6: Example of a Cloud Mask satellite product.

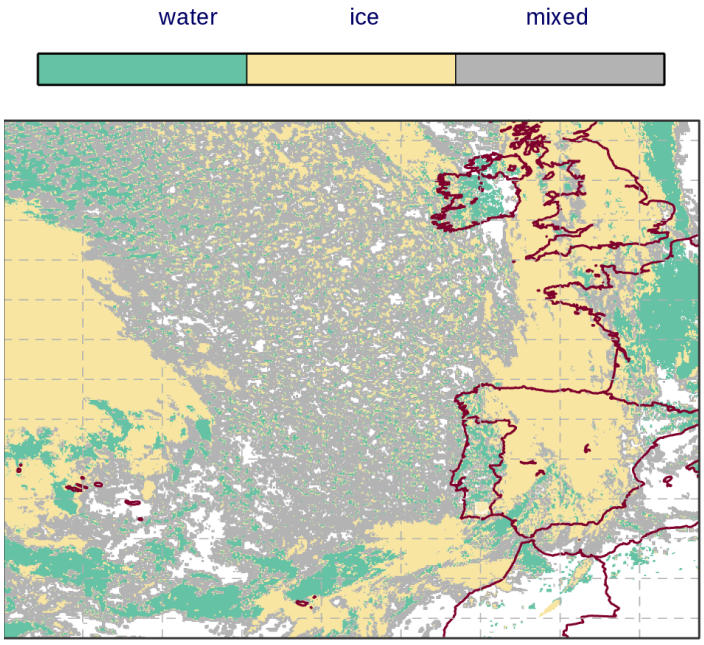

Figure 3.7: Example of a Cloud Phase satellite product. The white areas correspond to cloud free areas.

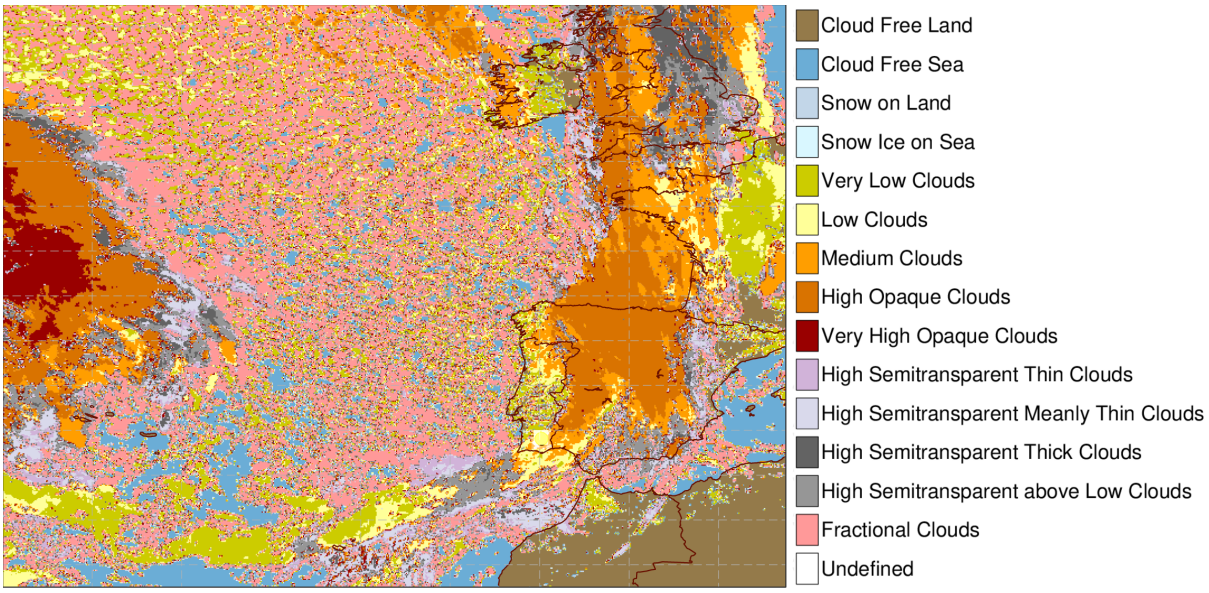

Figure 3.8: Example of a Cloud Type satellite product.

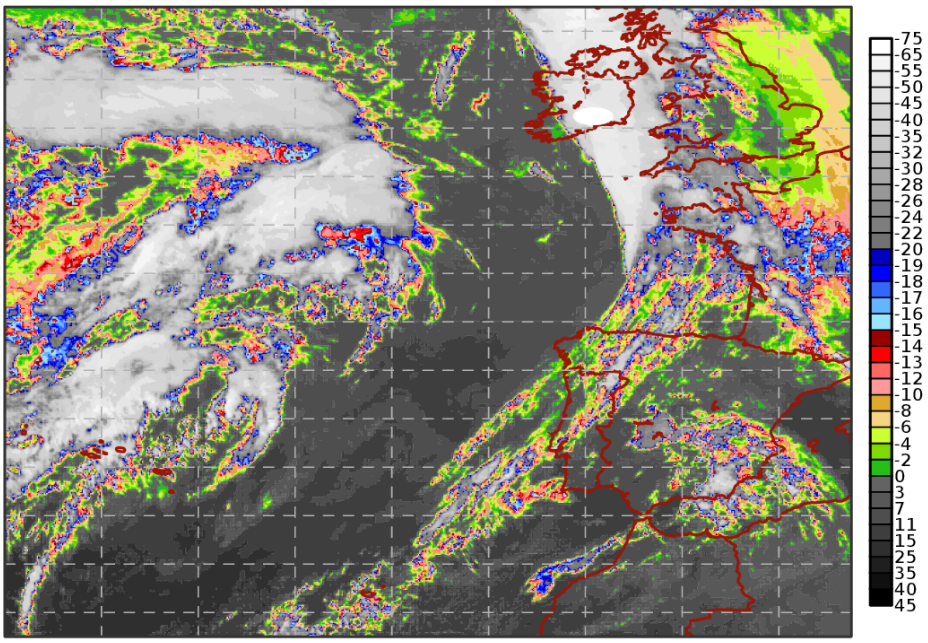

Figure 3.9: Example of a Brightness Temperature satellite product.

This analysis is focused in the region extending from $31°N$ to $57°N$ and $3°E$ to $32°W$, encompassing part of the paths of most flights to or from Portugal (mainland and islands), Spain, Britain and Ireland. The images captured on the same day and approximate hour of the PIREPs were considered.

3.3 Forecast Data

The forecast data is provided by the ECMWF deterministic model. Briefly, this model resolves a set of basic prognostic equations that describes the time evolution of the horizontal wind components, surface pressure, temperature and the water vapour content of the model atmosphere [58]. Besides, the model solves equations that describe physical processes within the atmosphere, such as changes in the hydrometeors (rain, snow, liquid water, cloud ice content, etc.). These model equations are discretized in space and time and solved numerically by a semi-Lagrangian advection scheme. The model uses also a cubic-octahedral spectral transform discretization, which corresponds to a grid spacing of approximately $9km$ [59].

The present model contains 137 vertical levels, the lowest level having a height of approximately $10m$ above the ground. In the troposphere, the vertical distance between vertical levels ranges from $20m$ close to the surface and $290m$ for altitudes above $6km$. In this work, three meteorological variables were considered, temperature (T), relative humidity (RH) and cloud water content (CWC), which consists of liquid water and ice. The model data of each variable was extracted to the nearest grid-point to the PIREP corrected location.

3.4 Methodology

As mentioned before, PIREPs are very useful in providing aircraft icing information, but they may contain errors in time and location attribution. Hence, considering that aircraft icing only occurs when clouds are present [17, 39], the satellite cloud mask was used to confirm the PIREPs location. Thus, at the pixel(s) nearest to the icing PIREP coordinates, cloud mask should be “partly cloudy” or “cloud filled”. After applying this verification, it was found that for 1.2% and 3.5% of the cases reported as moderate and severe icing, respectively, the satellite cloud mask was clear sky (see Figure 3.10). The PIREPs position errors can explain this. Thus, the PIREPs coordinates were slightly modified, so that the cloud mask of the corrected coordinates would be either partially cloudy or cloud filled. Two different statistical analysis were then made, one using the original coordinates of the icing PIREPs and other using the modified coordinates (see Tables 3.1 and 3.2). The lowest location error was $5km$ and the highest location error was $58km$.

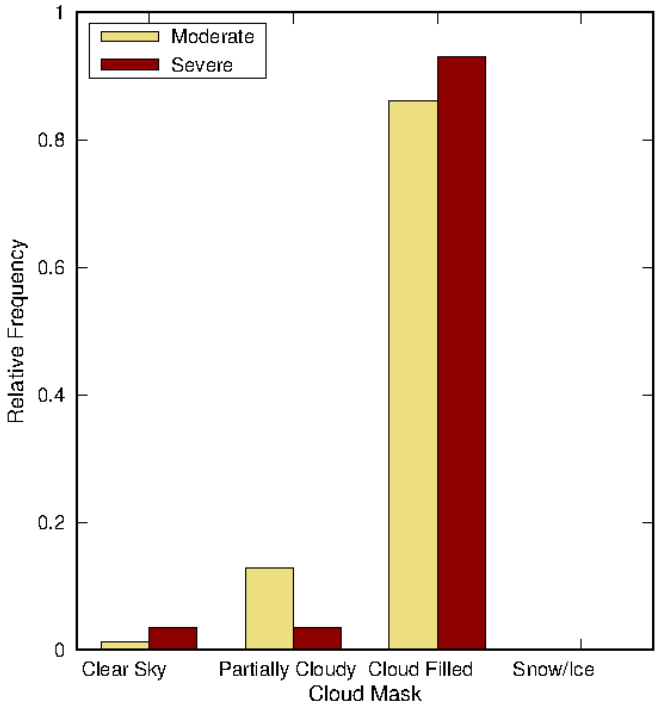

Figure 3.10: Distribution of the different types of cloud mask, for the aircraft icing pilot reports, for the original data.

Table 3.1: Characterization of the PIREPs that were slightly modified ('Orig.' - Original, 'Mod.' - Modified, 'Lat.' - Latitude, and 'Long.' - Longitude).

Severity	Date (yy.mm.dd)	Time (hh:mm)	Orig. Lat. (°)	Orig. Long. (°)	Mod. Lat. (°)	Mod. Long. (°)
moderate	2019.08.24	10:10	52.00	-8.00	51.95	-7.94
moderate	2020.08.28	18:15	39.78	-1.18	39.86	-1.14
moderate	2020.10.02	13:00	38.83	-0.35	38.91	-0.40
moderate	2020.10.03	06:00	41.02	-2.37	41.37	-2.48
moderate	2021.05.22	23:53	37.70	-24.55	37.60	-24.22
moderate	2022.03.01	10:30	38.73	-9.35	38.70	-9.30
severe	2020.02.26	10:48	51.83	-1.83	51.80	-1.74
severe	2021.05.13	08:35	40.37	-4.23	40.35	-3.54

Table 3.2: Characterization of the PIREPs that were slightly modified: location error (in distance, km) between the original and the modified coordinates (calculations made on [60]).

Severity	Date (yy.mm.dd)	Time (hh:mm)	Distance (km)
moderate	2019.08.24	10:10	7
moderate	2020.08.28	18:15	10
moderate	2020.10.02	13:00	10
moderate	2020.10.03	06:00	40
moderate	2021.05.22	23:53	31
moderate	2022.03.01	10:30	5
severe	2020.02.26	10:48	7
severe	2021.05.13	08:35	58

Chapter 4

Results and Discussion

This chapter begins by characterizing the overall results of this work, taking into account an overview of the studied region with the location of the selected PIREPs and the corresponding satellite products (cloud mask, cloud-top phase, cloud type and brightness temperature). Additionally, a statistic analysis of the satellite parameters associated to the aircraft icing reports will be considered. Moreover, a few case studies will be analyzed in detail.

4.1 Statistical Analysis

In this work, by matching up PIREPs and satellite products, i.e., satellite and meteorological fields for the same day and time of the reported aircraft icing events, the associated atmospheric conditions were studied.

4.1.1 Cloud Mask Analysis

Since clouds must be present for aircraft icing occur, it is expected that the selected PIREPs would be issued in a cloudy environment (i.e., with a cloud mask classification of partially cloudy or cloud-filled), which was verified, as mentioned before.

Besides the differences between the original and the screened events, explained by the position errors in PIREPs, the majority of the severe icing events occurred in a cloud-filled environment: 93.1% for the original data (Figure 3.10) and 96.6% for the modified data (Figure 4.1). The percentage of cloud-filled prevails also for the moderate icing events, but with lower percentages, 86.1% and 88.4%, respectively, for the original and modified data (compare Figures 3.10 and 4.1). This result is coherent with former studies (Politovich [44] and Cober et al. [35]), revealing that even though most of the aircraft icing cases occur in a cloud-filled environment, partially cloudy conditions may also lead to aircraft icing phenomena.

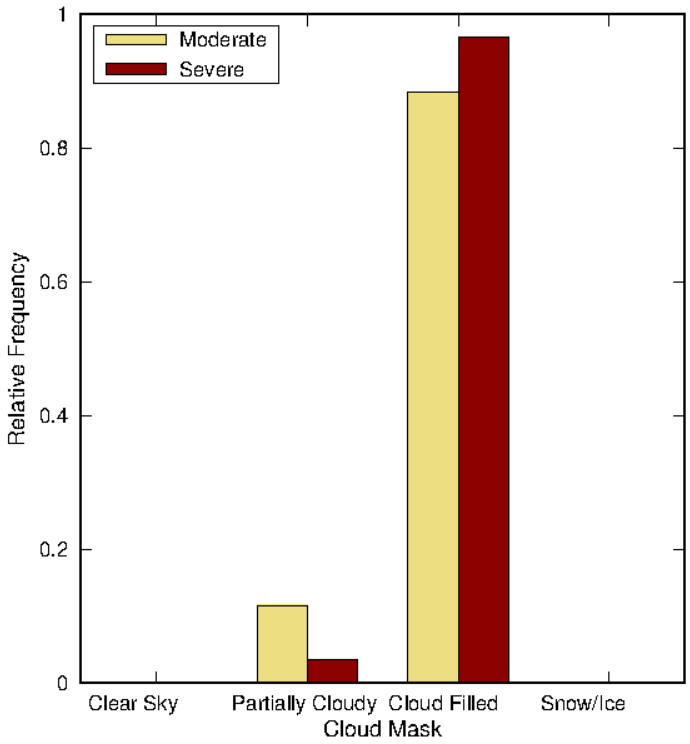

Figure 4.1: Distribution of the different types of cloud mask, for the aircraft icing pilot reports, for the modified data.

4.1.2 Cloud-top Phase Analysis

Figure 4.2 (a) displays the geographical distribution of the cloud-top phase product associated with each aircraft icing event in the studied region. In the Iberian Peninsula, most of the PIREPs are associated with a cloud-top phase of ice, followed by mixed-phase and water (see Figure 4.2 (b)). In the regions of England, Wales and Republic of Ireland, the percentage of water cloud-top phase is higher than in Iberia (compare with Figure 4.2 (c)), probably because the icing events in Iberia tend to occur at higher heights (see section 3.1). Figure 4.3 shows that almost 60% of moderate icing events occurred in a cloud environment with ice cloud-top phase, followed by 30.2% and 11.6% with mixed and water, respectively. On the other hand, for severe icing events, the cases of ice and mixed cloud-top phases have a similar prevalence, approximately 38% and 41%, respectively. It should be noted that the cloud phase identified in the satellite products is most likely the phase of the upper cloud layers, while the PIREPs may have happened at lower altitude. The temperature and, hence, the cloud phase at the reported altitude may be different than the ”cloud-top” phase. The high number of cases with mixed cloud-top phase is consistent with previous studies like in Korolev et al. [22].

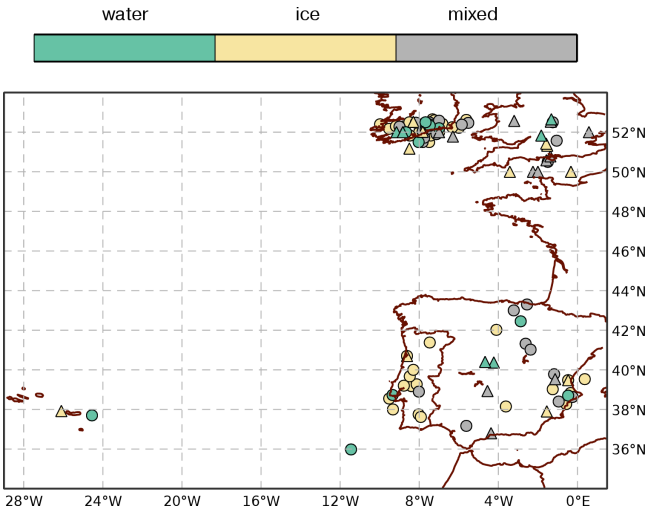

(a) Western Europe and Northeastern Atlantic sector.

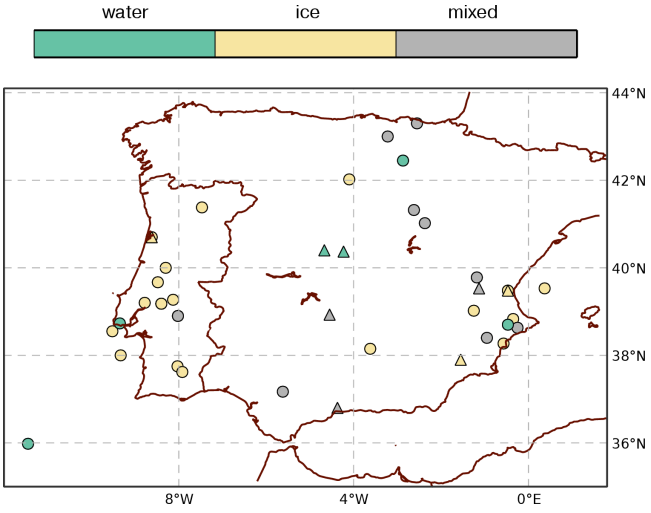

(b) Zoom in of Iberian Peninsula.

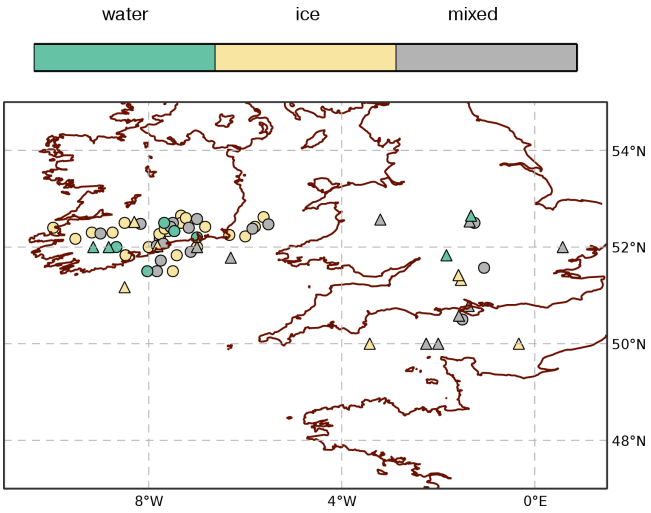

(c) Zoom in of England, Wales and Republic of Ireland.

Figure 4.2: Cloud-top Phase satellite product at the locations of the aircraft icing reports (circles and triangles refer to moderate and severe icing, respectively), at Western Europe and Northeastern Atlantic sector (a), Iberian Peninsula (b) and England, Wales and Republic of Ireland (c).

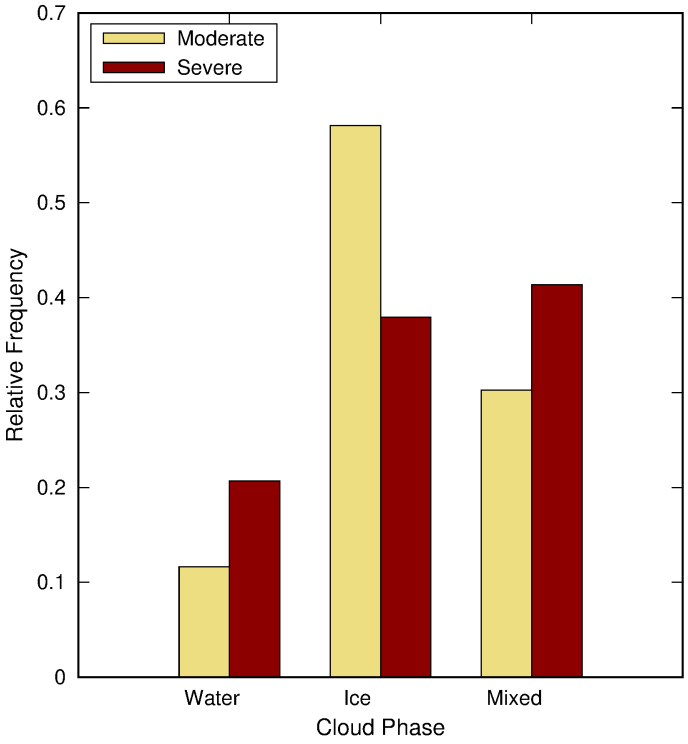

Figure 4.3: Relative frequency of different types of Cloud-top Phase for the aircraft icing events.

4.1.3 Cloud Type Analysis

The geographical distribution of the cloud type associated with the aircraft icing events is depicted in Figure 4.4. The majority of the aircraft icing events occurred under the presence of medium and high opaque clouds (see Figures 4.4 (b) and (c) for a more detailed view). Few cases were associated with low clouds and high semitransparent clouds. As expected there were no cases in the presence of fractional clouds or in a cloud-free environment (pre-screened).

The histogram presented in Figure 4.5 reveals that for moderate icing almost 40% of the events occurred under high opaque clouds, followed by 26.7% and 10.5% in medium and very high opaque clouds, respectively. For severe icing, most events were associated with medium and high opaque clouds, accounting for about 78% of total cases, while 10.3% were associated with low clouds. Figure 4.5 also shows a small percentage of aircraft icing events associated with high semitransparent clouds. This result is not surprising, since the temperatures in these clouds are much lower than the typical temperatures prone to aircraft icing conditions [30, 33, 35]. Nevertheless, supercooled water droplets may be present in cirrus clouds [61]. Moreover, the icing events associated with high clouds may have occurred within other types of clouds that may have been formed beneath these clouds but cannot be detected by these satellite products [39, 57].

Resorting to the classification system mentioned in section 2.1.3, it was possible to calculate an approximate range of temperatures associated to each cloud group for middle latitudes, where the studied region is inserted (see Table 4.1). These scenarios were constructed for a standard atmosphere, which assumes a two-meter temperature (T2m) of $15°C$ and for the months with greater icing PIREPs' fre-

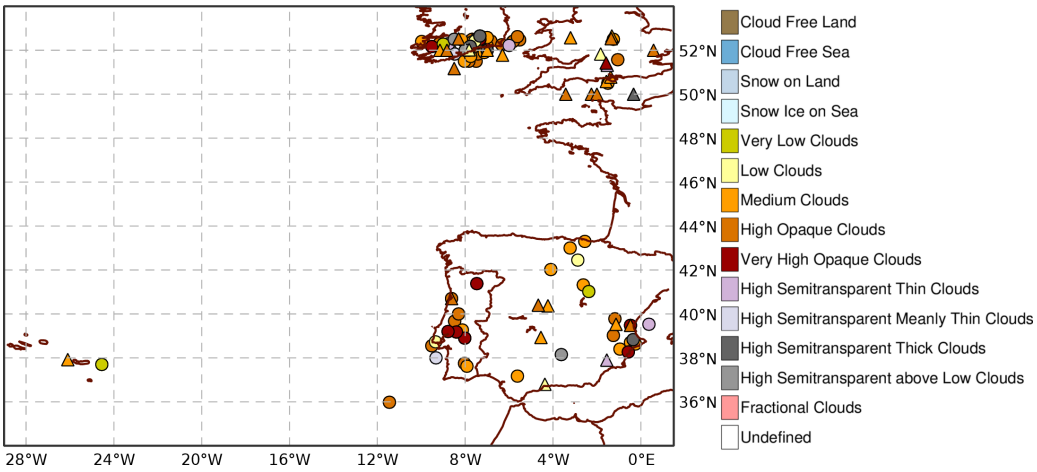

(a) Western Europe and Northeastern Atlantic sector.

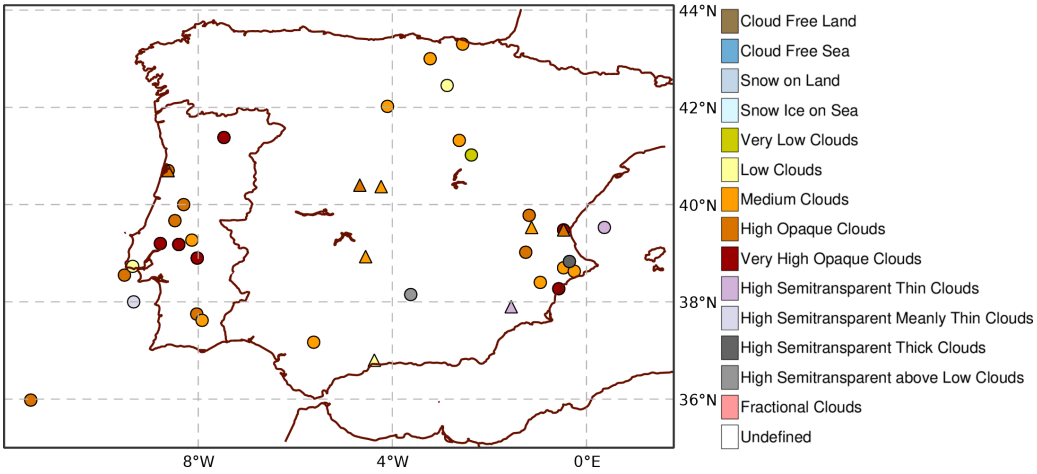

(b) Zoom in of Iberian Peninsula.

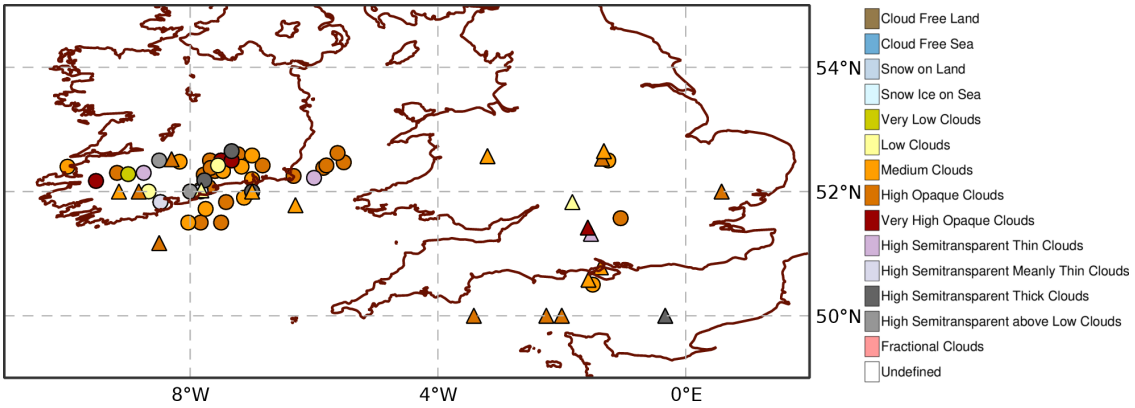

(c) Zoom in of England, Wales and Republic of Ireland.

Figure 4.4: Cloud Type satellite product at the locations of the aircraft icing reports (circles and triangles refer to moderate and severe icing, respectively), at Western Europe and Northeastern Atlantic sector (a), Iberian Peninsula (b) and England, Wales and Republic of Ireland (c).

quency, namely October (the average T2m is $11°C$ in London and $18°C$ in Lisbon) and December (the average T2m is $5.6°C$ in London and $11°C$ in Lisbon [53]), assuming a lapse rate of $6.5°C/km$. Note that the categories of very low and very high opaque clouds derived from the satellite cloud type product are assumed to be included in the low and high clouds groups, respectively. Referring to Table 4.1, it is

noticeable that middle and high clouds develop in an environment with temperatures where theoretically aircraft icing may form (between -40 and $0°C$ [27, 28]); furthermore, middle clouds temperatures fall in the range where aircraft icing is mostly likely to occur (between -20 and $0°C$ [27, 28, 38, 39]). Therefore, it is expected that most of the icing events are associated mainly with middle clouds, followed by high clouds. Also, for warmer climates (see the last two rows from Table 4.1), aircraft icing can occur at higher altitudes.

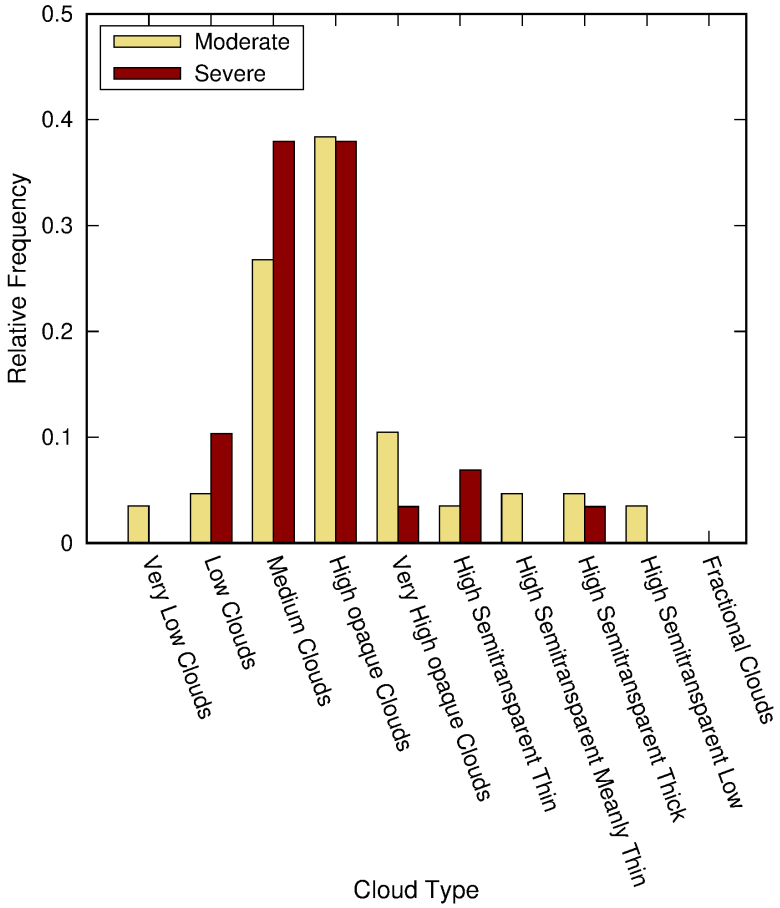

Figure 4.5: Relative frequency of different types of Cloud Type for the aircraft icing events.

Table 4.1: Approximate range of temperatures associated to each cloud group. The months with greater icing PIREPs' frequency were used: October (the average T2m is $11°C$ in London and $18°C$ in Lisbon) and December (the average T2m is $5.6°C$ in London and $11°C$ in Lisbon). The standard atmosphere was also used (T2m: $15°C$) and a lapse rate of $6.5°/km$.

Cloud Group	Low	Middle	High
Cloud's Base Height	0 to 6560 ft	6560 to 22970 ft	16400 to 42650 ft
Average T2m 5.6°C	5.6 to -7.4°C	-7.4 to -39.9°C	-26.9 to -78.9°C
Average T2m 11°C	11 to -2°C	-2 to -34.5°C	-21.5 to -73.5°C
Average T2m 15°C	15 to 2°C	2 to -30.5°C	-17.5 to -69.5°C
Average T2m 18°C	18 to 5°C	5 to -27.5°C	-14.5 to -66.5°C

4.1.4 Brightness Temperature Analysis

It should be emphasized that it is considered the cloud top temperature to be closely represented by the $10.8\mu m$ (within the thermal infrared atmospheric window) brightness temperature provided by the MSG satellite. This assumption has some limitations and the following aspects should be contemplated [62]:

1. The greater the cloud top height, the scarcer will be the atmosphere between the cloud top and the satellite sensor, i.e., the transmissivity of the atmosphere in the atmospheric window becomes very high (acting as a transparent means between the cloud top and the sensor) and, therefore, the more reliable is the approximation. This is the case for, e.g., cloud tops with an altitude above approximately $7km \approx 23000ft$ (corresponding to a FL230). Conversely, for lower altitudes the cloud top temperature may be underestimated. However, the thermal infrared channel used, $10.8\mu m$, is less sensitive to the effect of atmospheric gases (the absorption of water vapor, $\mathrm{CO_2}$ and $\mathrm{O_3}$ in this band of the electromagnetic spectrum is relatively low), so the approximation remains valid for medium cloud tops.

2. The problematic situations occur in the presence of semi-transparent or/and fractional clouds. In these cases, part of the received signal by the satellite is emitted and reflected by the surface, so there will be likely an overestimation of the cloud top temperature. However, these cases are not of interest in this work. Also in the case of low warm clouds, an atmospheric correction may be necessary to apply, since a thicker atmosphere above (longer optical path) reduces transmissivity. Nevertheless, even in these cases, the correction should be small and only above $5°C$ for very moist above-cloud atmospheres.

3. The cloud top emits radiation, following the Planck's law, with an emissivity below 1 (but very close to 1, in the $10.8\mu m$), since it is not a black-body. Here the emissivity effect is ignored, assuming that the brightness temperature in the $10.8\mu m$ channel corresponds to the cloud top temperature. Nevertheless, the errors introduced are marginal, validating the use of the brightness temperature of the thermal infrared $10.8\mu m$ channel as an approximation of cloud top temperature.

Figure 4.6 (a) displays the geographical distribution of the $10.8\mu m$ brightness temperature (BT10.8) at the time of each aircraft icing event within the studied region. This figure suggests that a significant amount of the icing occurrences took place with BT10.8 between $-40°C$ and $-19°C$, followed by BT10.8 in the range of $-19°C$ and $-2°C$ (see Figures 4.6 (b) and (c) for a more detailed view). The histogram depicted in Figure 4.7 reveals that the majority of the icing events ($\approx 70\%$) occurred with BT10.8 between $-40°C$ and $-8°C$. Moreover, nearly 19% of moderate icing and 10% of severe icing were associated with BT10.8 between $-56°C$ and $-40°C$. Previous studies, as in Curry et al. [41], have shown that 99% of the icing occurrences associated with medium clouds fall in the temperature range of $-36°C$ and $-2°C$. Two facts may explain the difference between these results. First, in the present study, over 40% of the icing occurrences were associated with high or very high opaque clouds. Secondly, Curry et al. [41] estimated the cloud temperature using satellites products and NWP analyses, whereas, in the present

study, BT10.8 is a proxy of the cloud top temperature, which may be lower than the temperature where the aircraft icing occurred.

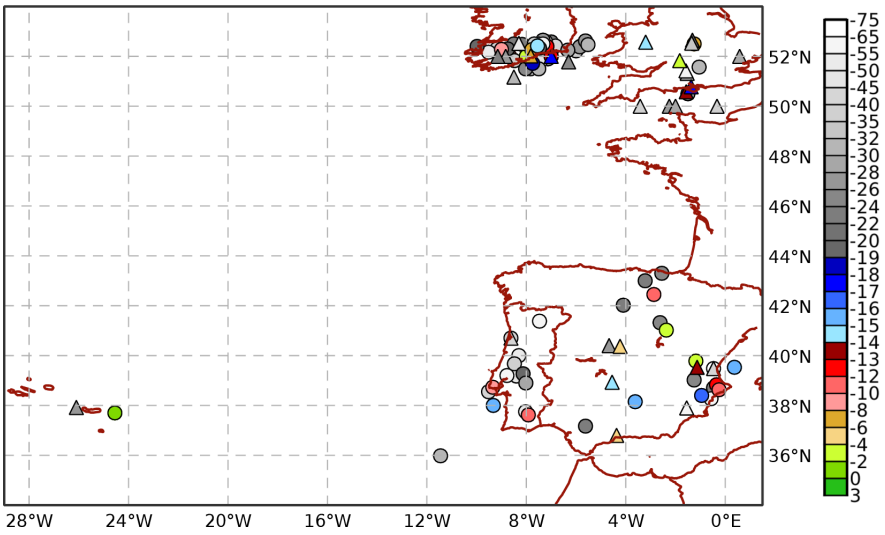

(a) Western Europe and Northeastern Atlantic sector.

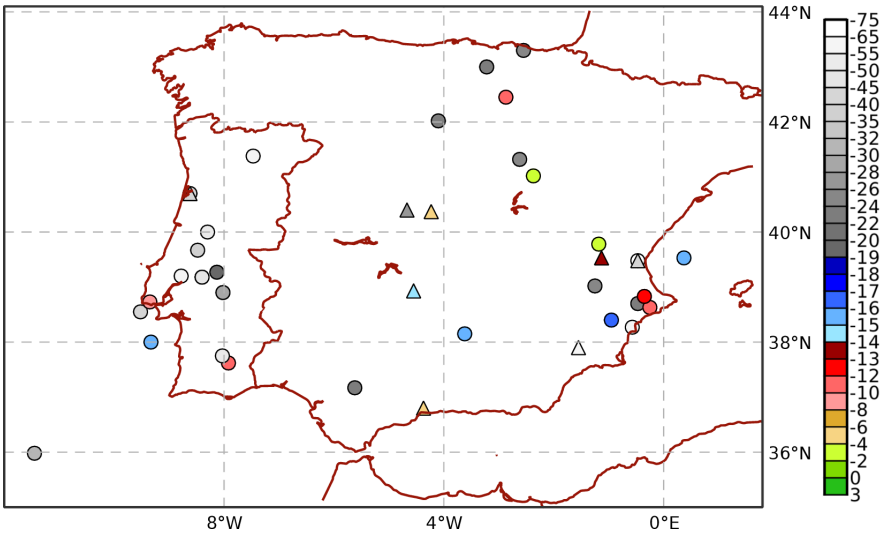

(b) Zoom in of Iberian Peninsula.

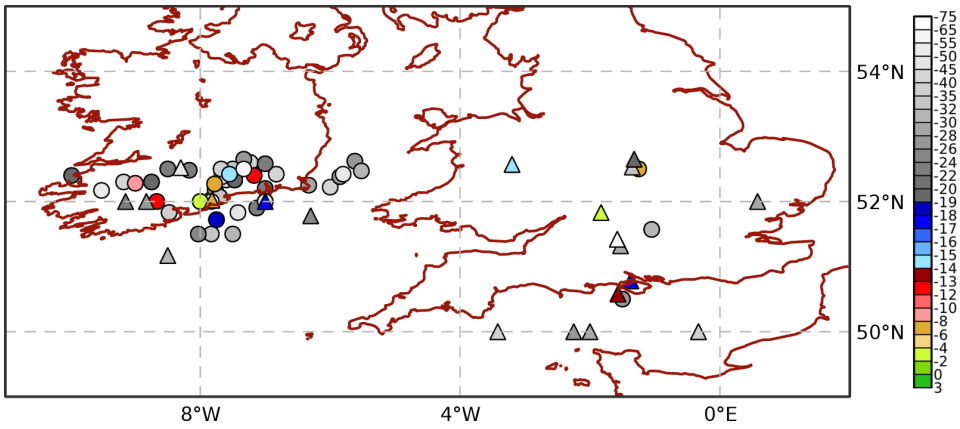

(c) Zoom in of England, Wales and Republic of Ireland.

Figure 4.6: BT10.8 satellite product at the locations of the aircraft icing reports (circles and triangles refer to moderate and severe icing, respectively), at Western Europe and Northeastern Atlantic sector (a), Iberian Peninsula (b) and England, Wales and Republic of Ireland (c).

Figure 4.7 also reveals that one moderate icing event occurred with a positive BT10.8 ($1.4°C$). This result can be associated with two scenarios. First, if an aircraft has been in below-freezing temperatures and then traverses an environment with above-freezing temperatures, the surface temperature of the aircraft may remain below freezing for some time. Therefore, aircraft icing can occur at slightly positive temperatures. Another possible scenario is the presence of a temperature inversion. After resorting to its pilot report and temperature data from the ECMWF model, a temperature inversion was indeed identified in the ECMWF profile associated with a very low cloud (according to the cloud type product classification), where the ECMWF temperature was $-0.8°C$ at FL070 (see Figure A.1 in Appendix A).

Figure 4.7 also shows that for BT10.8 within the range between -4 and $0°C$ and -28 and $-12°C$, severe icing (accounting to 66%) is more frequent than moderate icing. The higher frequency for temperatures below $-4°C$ is consistent with previous studies showing that the liquid water content decreases as temperatures decreases, while the concentration of ice particles increases as the temperature decreases (Hu et al. [63]). Furthermore, the formation of large supercooled droplets is favored for clouds with relatively warm tops (warmer than $-15°C$), since high ice concentrations, which can deplete supercooled liquid water, are not fostered in this environment [44].

Lastly, comparing Figures 4.7 and A.2 (presented in Appendix A), it is noticeable that, using the data with the uncorrected coordinates, there are a few icing occurrences with BT10.8 above $0°C$. After the slight correction of the PIREPs coordinates (see section 3.1) this was not verified (except for one case previously mentioned). This is consistent with prior studies (Kane et al. [64]).

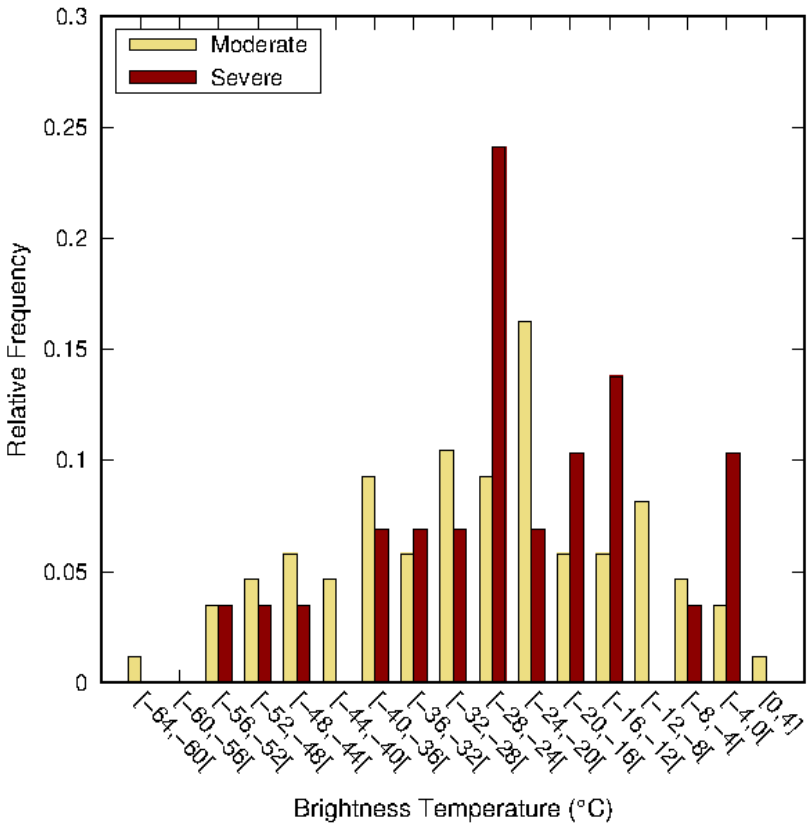

Figure 4.7: Relative frequency of different values of BT10.8, for the aircraft icing events, for the modified data.

4.1.5 Relation between Cloud Phase and Brightness Temperature

For a better comprehension of the atmospheric conditions present during the studied icing events, it was performed a statistical analysis of the BT10.8 distribution associated with cases where the cloud-top phase was classified as water (Figure 4.8) and ice (Figure 4.9). For aircraft icing events with a cloud-top phase classified as "water", the moderate cases show a broad distribution with BT10.8 values ranging between -34 and $2°C$. For severe icing, BT10.8 reveals a bi-modal distribution with one maximum frequency (almost 70%) between -26 and $-18°C$, and a second peak (approximately 32%) between -6 and $2°C$. For events with a cloud-top phase classified as "ice", the majority of the moderate icing occurrences ($> 70\%$) are associated with BT10.8 between -56 and $-8°C$ and, more specifically, almost 66% between -52 and $-24°C$. For severe icing, almost 64% of the cases took place in an environment characterized by BT10.8 ranging from -40 to $-24°C$. These results are consistent with other studies, which have shown that the fraction of ice particles is low for temperatures between $-10°C$ and $0°C$ (Hu et al. [63]) and that the fraction of water particles decreases for colder temperatures down to $-40°C$ (Korolev et al. [22]). Moreover, Isaac et al. [24] found that cumulus clouds with tops warmer than $-8°C$ did not contain ice. Comparing Figures 4.8 and 4.9, it is clear that clouds with a cloud-top composed of water are characterized by higher BT10.8 (minimum of $-34°C$) than clouds with a cloud-top phase of ice (minimum of $-64°C$), as suggested by previous works [23, 24].

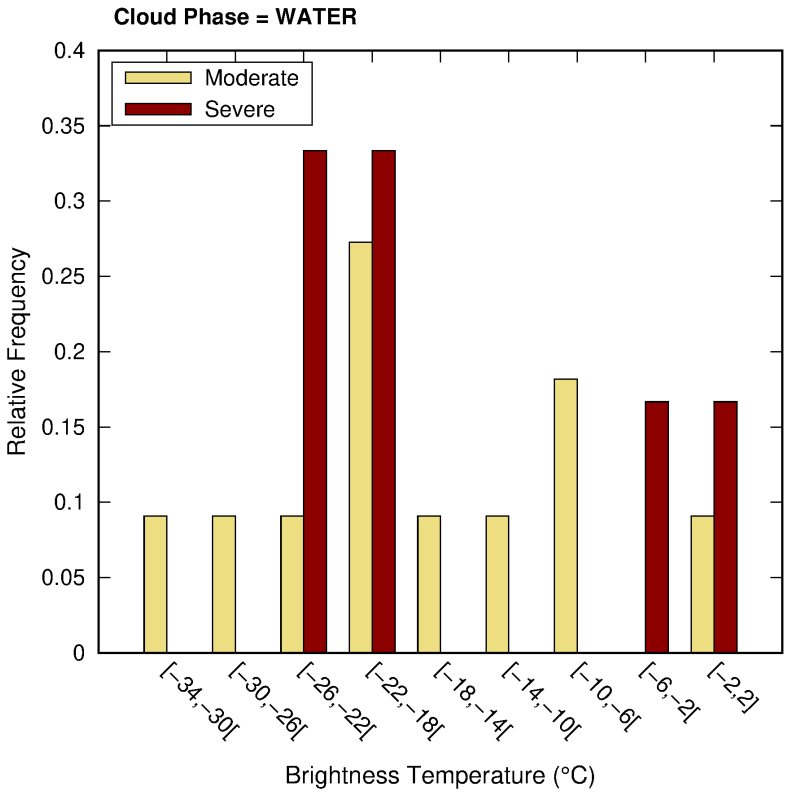

Figure 4.8: BT10.8 distribution associated with the events where the cloud-top phase was classified as water.

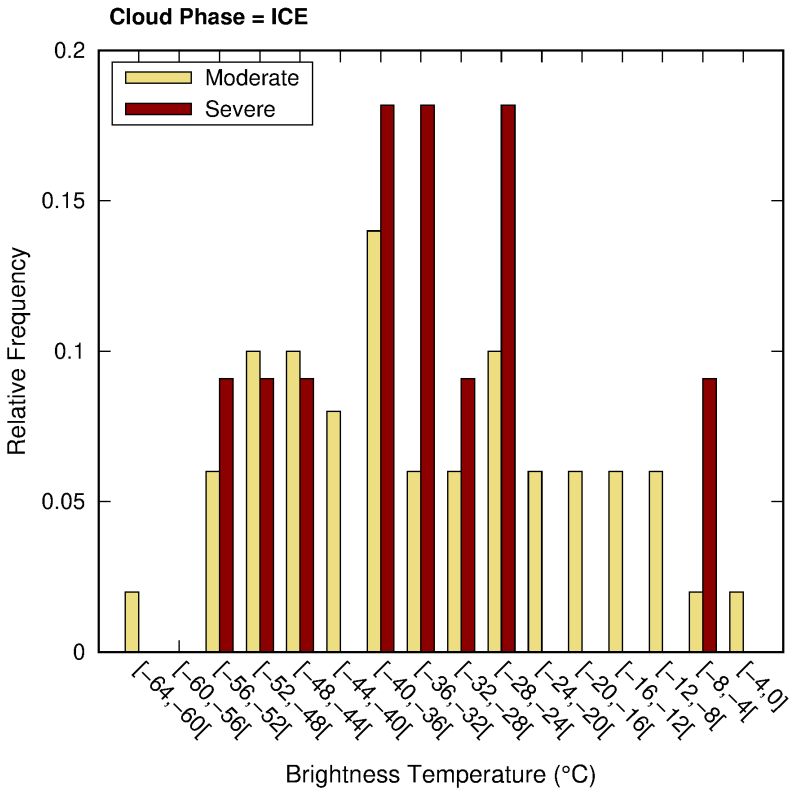

Figure 4.9: BT10.8 distribution associated with the events where the cloud-top phase was classified as ice.

4.2 Specific Cases Analysis

To better understand the meteorological conditions associated to the sample of aircraft icing events, a more exhaustive and detailed study will be realized. Accordingly, four case studies will be considered, 3 of severe and 1 of moderate icing. Note that the PIREPs of each case are represented in the following maps with the red solid circle for the severe icing events, and orange and magenta solid circles for the moderate icing occurrence.

4.2.1 Severe icing Case - 1 March 2019

Figure 4.10 displays the geographical distribution of cloud type, BT10.8 and cloud-top phase at 1930 UTC on 1 March 2019, when a PIREP of severe icing was issued in Ireland. High opaque clouds are noticeable in the region (Figure 4.10 (a)), with ice near the cloud top and a BT10.8 of around -47 to $-48°C$ (Figure 4.10 (b) and (c)). A band of very low clouds with warmer ($> 0°C$) cloud tops can be seen to the west of the former. These clouds are also characterized by the presence of water-phase at the cloud top (Figure 4.10 (c)).

Figure 4.11 shows the vertical profile of temperature, RH and CWC from the ECMWF model at the nearest grid-point of the PIREP location. Bearing in mind the temperatures at which aircraft icing may happen (between $-40°C$ and $0°C$), this icing event could have occurred between FL60 and FL260 (see Figure 4.11 a)). The reported flight level of the icing event was FL230 which corresponds to a

temperature forecast of about $-33°C$, while the flight level corresponding to the BT10.8 observed value is approximately FL284. The vertical profiles of CWC and RH (Figure 4.11 b)) suggest the presence of three layers of clouds when this PIREP was issued (a threshold of $0.02 g/kg$ was used for the CWC, and a threshold of 90% was used for the RH [9]): one layer of high clouds between FL200 and FL310, and two layers of lower clouds underneath it. Thus, the highest cloud layer predicted by the ECMWF model overlaps the clouds identified in the satellite observations and the region where the PIREP was issued (FL230). Furthermore, the comparison between model and satellite data suggests that the aircraft icing event occurred in a cloud located between FL200 and FL284 and that the model overestimates the cloud top. The icing event was associated with a CWC of $0.06 g/kg$ and a RH of 92.7%, according to the ECMWF model.

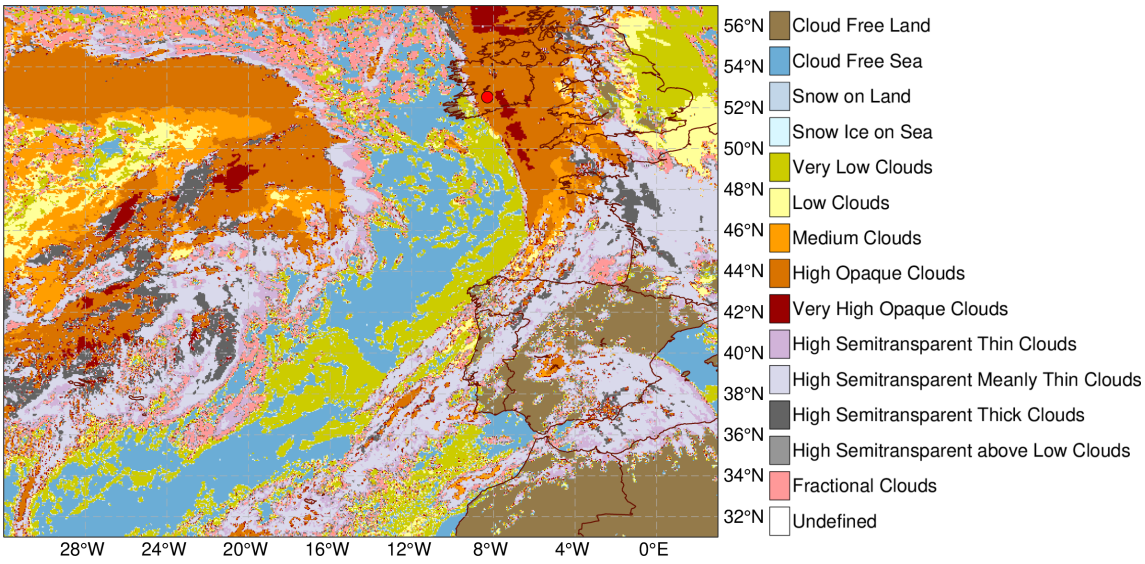

(a) Cloud Type.

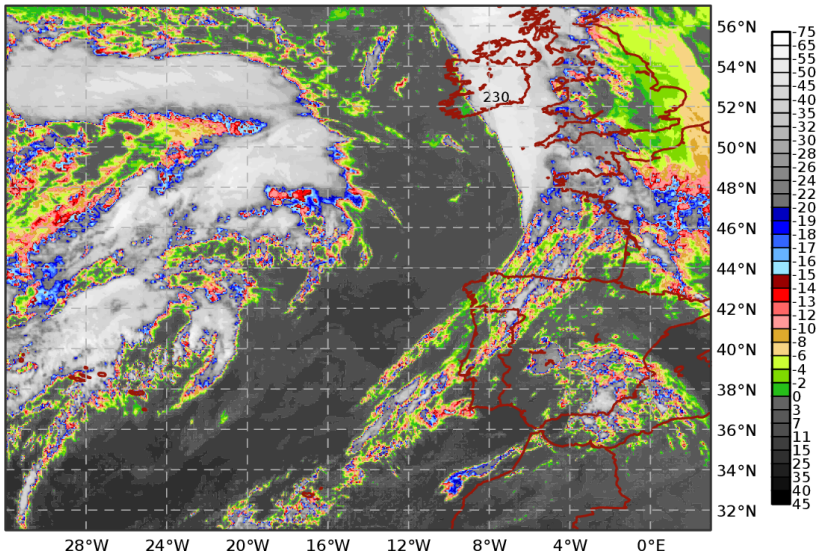

(b) $10.8 \mu m$ Brightness Temperature.

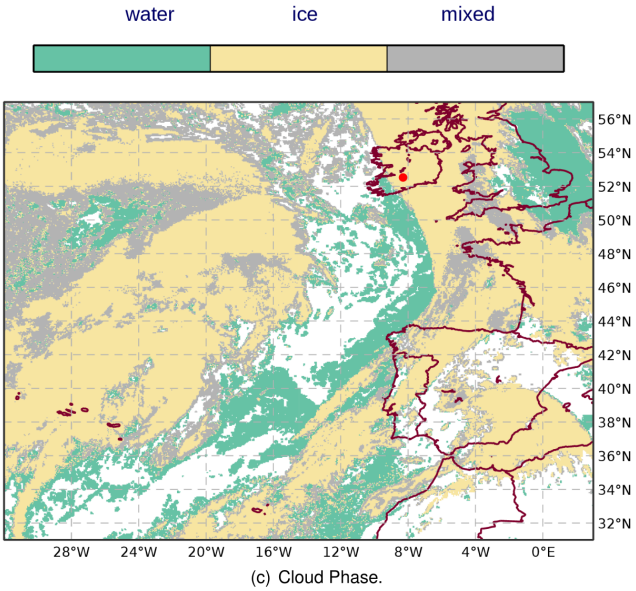

Figure 4.10: Satellite products valid at 1930 UTC on 1 March 2019. The location of the pilot report of severe icing is represented with a red solid circle in the cloud type (a) and cloud-top phase product (c), and with the FL value in the BT10.8 product (b). The white areas correspond to cloud free areas in the cloud-top phase product (c).

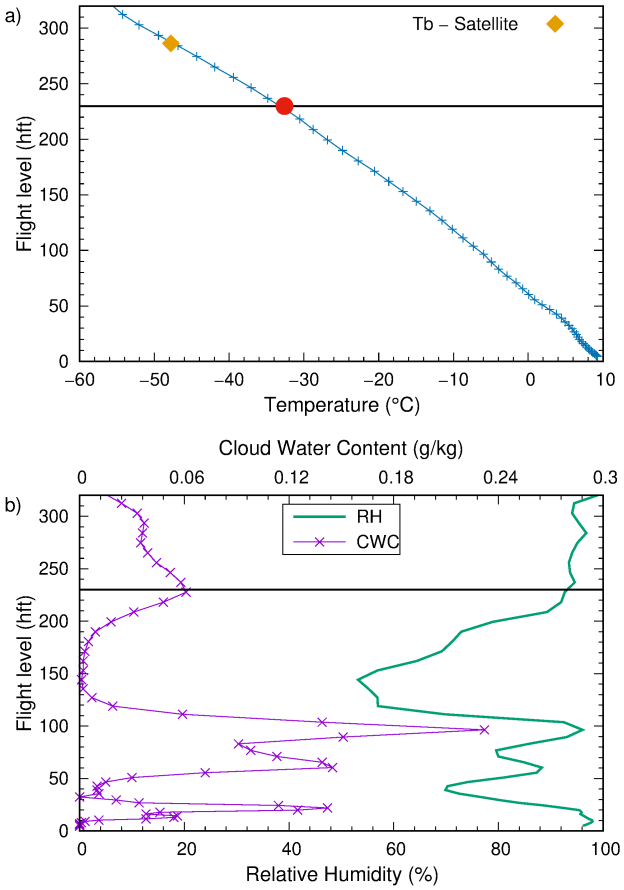

Figure 4.11: Vertical profile of (a) temperature (the red solid circle represents the temperature at the reported altitude of the icing PIREP) and (b) CWC and RH. The black solid line represents the FL230. The profiles are obtained from the European Centre for Medium-Range Weather Forecasts (H+7) from 1930 UTC on 1 March 2019.

4.2.2 Severe icing Case - 7 June 2019

Figure 4.12 displays the geographical distribution of cloud type, BT10.8 and cloud-top phase at 0600 UTC on 7 June 2019, when a PIREP of severe icing was issued south of England, in the English Channel. High opaque clouds are noticeable in the region (Figure 4.12 (a)). These clouds have a BT10.8 of about -24 to $-25°C$ (Figure 4.12 (b)) and a cloud-top composed of ice (Figure 4.12 (c)). South of this region, over Biscay Gulf, medium, low and very low clouds with warmer cloud tops are visible. These clouds are also characterized by the presence of mixed and water-phase in the cloud top (Figure 4.12 (c)).

Figure 4.13 shows the vertical profile of temperature, RH and CWC from the ECMWF model at the nearest grid-point of the PIREP location. Considering the temperatures that favour aircraft icing, this icing event could have occurred between FL073 and FL275 (see Figure 4.13 a)) and most likely between FL073 and FL195, where temperature varies between $-20°C$ and $0°C$. The reported flight level was FL160, corresponding to a temperature forecast of about $-13°C$, considerably warmer than the BT10.8. The corresponding flight level of the BT10.8 is approximately FL216. The ECMWF vertical profiles of CWC and RH (Figure 4.13 b)) indicate the presence of one thick cloud layer when this PIREP was issued (a threshold of $0.02g/kg$ was used for the CWC, and a threshold of 90% was used for the RH [9]) between FL035 and FL320. Thus, the comparison between model and satellite data suggests that the icing event occurred within a thick cloud, beneath the cloud top (FL216) and that again the model overestimates the cloud top. The icing event was associated with a CWC near $0.18g/kg$ and a RH of almost 100%, according to the ECMWF model.

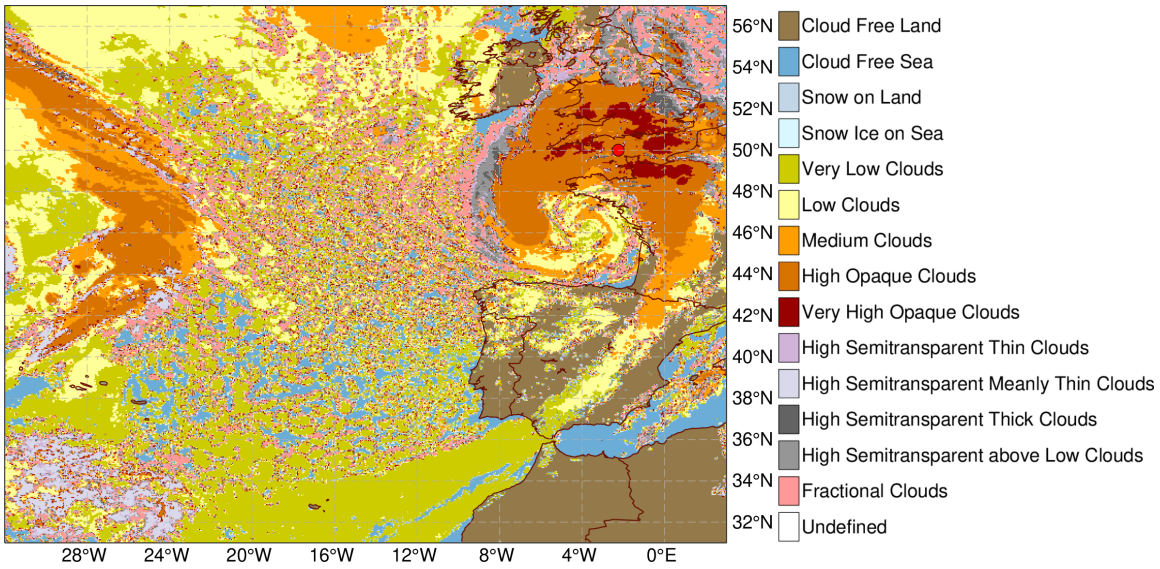

(a) Cloud Type.

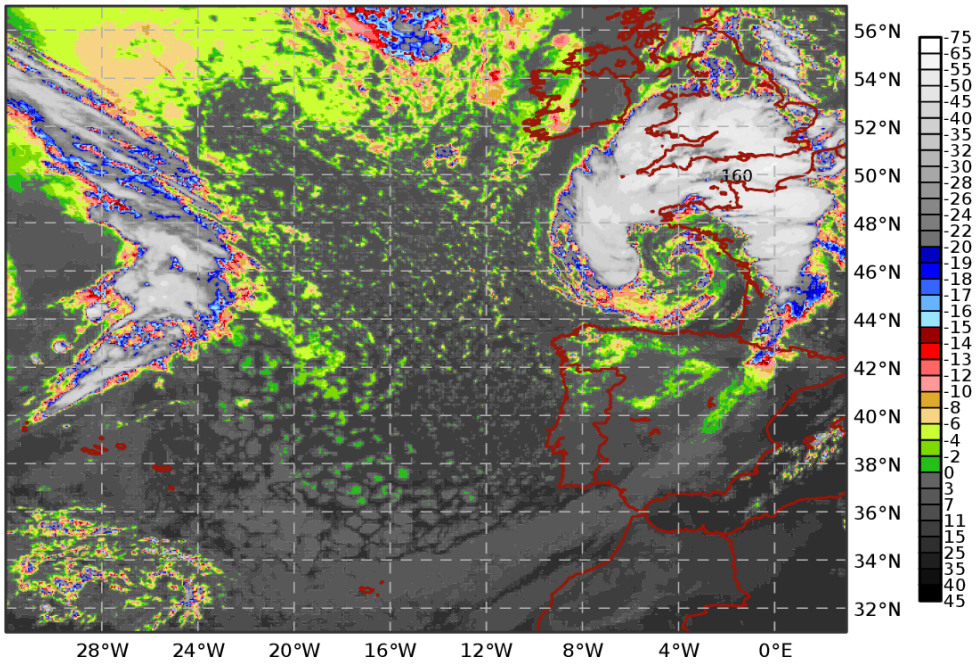

(b) $10.8\mu m$ Brightness Temperature.

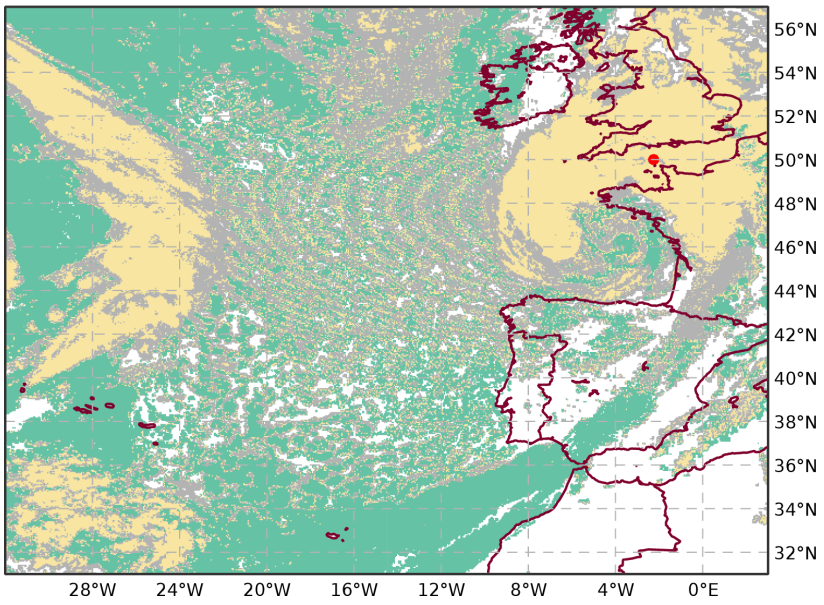

(c) Cloud Phase.

Figure 4.12: Satellite products valid at 0600 UTC on 7 June 2019. The location of the pilot report of severe icing is represented with a red solid circle in the cloud type (a) and cloud-top phase product (c), and with the FL value in the BT10.8 product (b). The white areas correspond to cloud free areas in the cloud-top phase product (c).

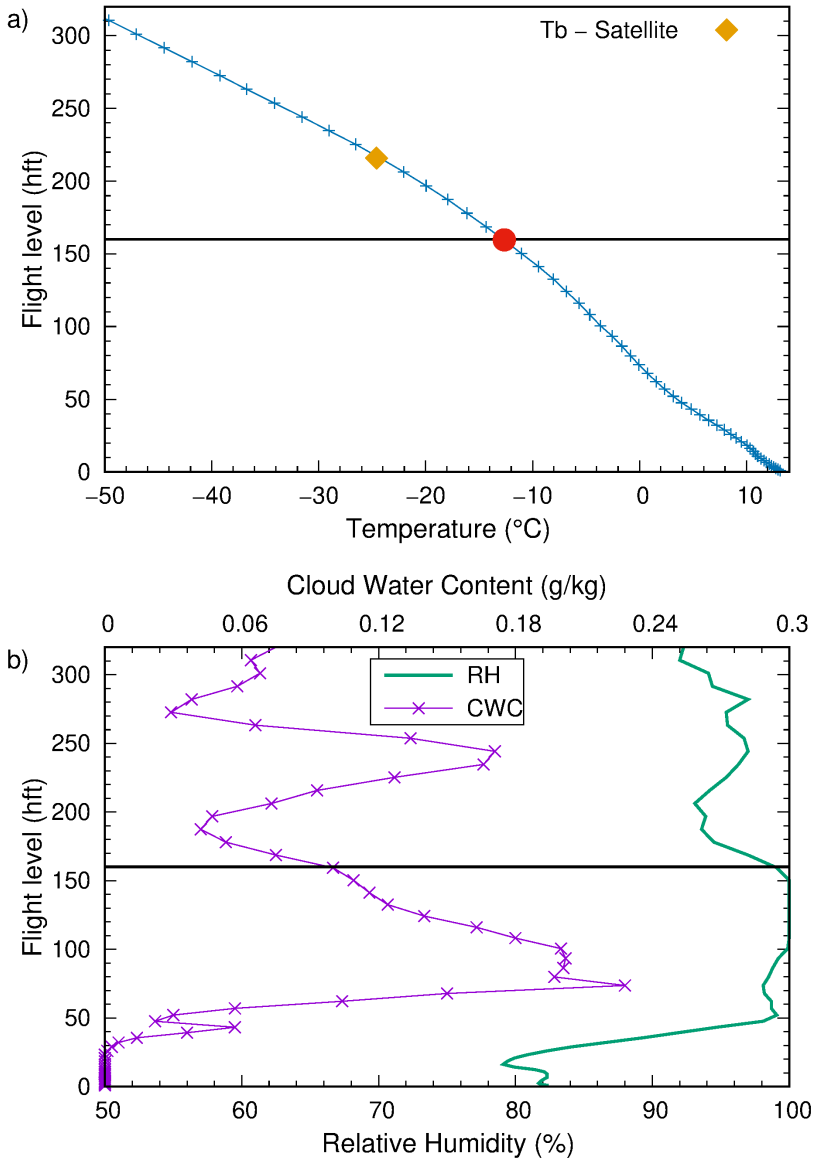

Figure 4.13: Vertical profile of (a) temperature (the red solid circle represents the temperature at the reported altitude) and (b) CWC and RH. The black solid line represents the FL160. The profiles are obtained from the European Centre for Medium-Range Weather Forecasts (H+6) from 0600 UTC on 7 June 2019.

4.2.3 Severe icing Case - 26 February 2020

Figure 4.14 displays the geographical distribution of cloud type, BT10.8 and cloud-top phase at 1045 UTC on 26 February 2020, when a PIREP of severe icing was issued in England. Low clouds are noticeable in the region (Figure 4.14 (a)), with a BT10.8 of about $-4°C$ (Figure 4.14 (b)) and a cloud-top composed of water droplets (Figure 4.14 (c)), as expected from other studies [43] at these temperatures. Near these clouds, very low clouds, some with warmer ($> 0°C$) cloud tops, are visible.

Figure 4.15 shows the vertical profile of temperature, RH and CWC from the ECMWF model at the nearest grid-point of the PIREP location. This temperature profile suggests that this icing event could have occurred between FL023 and FL220 (see Figure 4.15 a)). The flight level of the icing PIREP was FL035 which corresponds to a temperature forecast of about $-3°C$. The corresponding flight level of the BT10.8 is approximately FL040, closely above the FL of the PIREP, suggesting that this icing event occurred near the cloud top. The vertical profiles of CWC and RH (Figure 4.15 b)) show the presence of one low cloud layer between FL040 and FL060, where RH is above 90% and CWC reaches a maximum value of $0.09g/kg$. Below FL040, the CWC is zero and RH decreases to values between 80 and 60%. Thus, although the model was able to predict the presence of a low cloud, it overestimated its cloud-top height by about $20hft$.

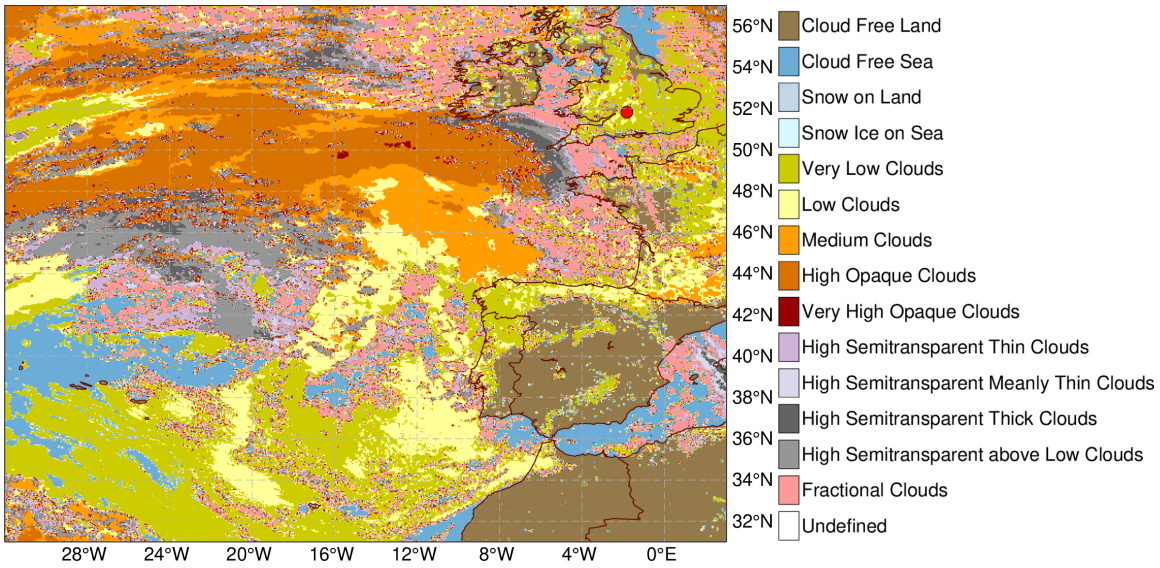

(a) Cloud Type.

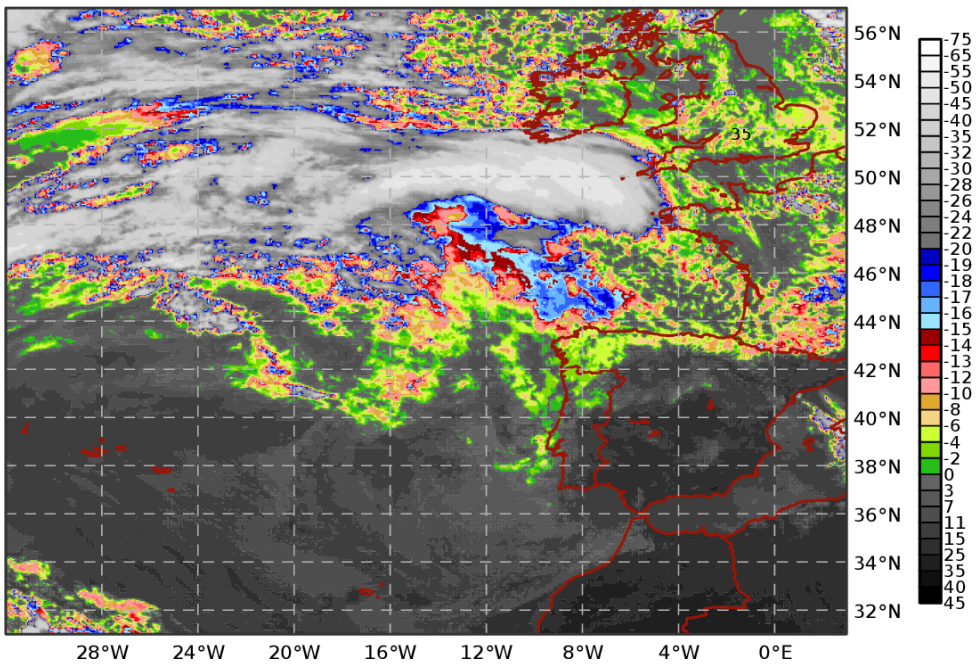

(b) $10.8\mu m$ Brightness Temperature.

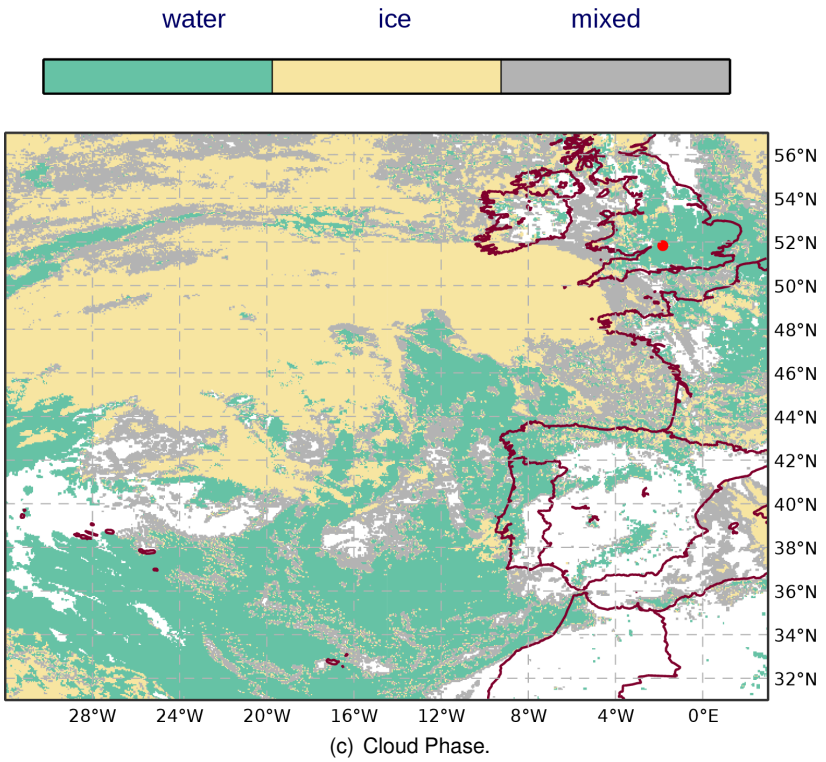

(c) Cloud Phase.

Figure 4.14: Satellite products valid at 1045 UTC on 26 February 2020. The location of the pilot report of severe icing is represented with a red solid circle in the cloud type (a) and cloud-top phase product (c), and with the FL value in the BT10.8 product (b). The white areas correspond to cloud free areas in the cloud-top phase product (c).

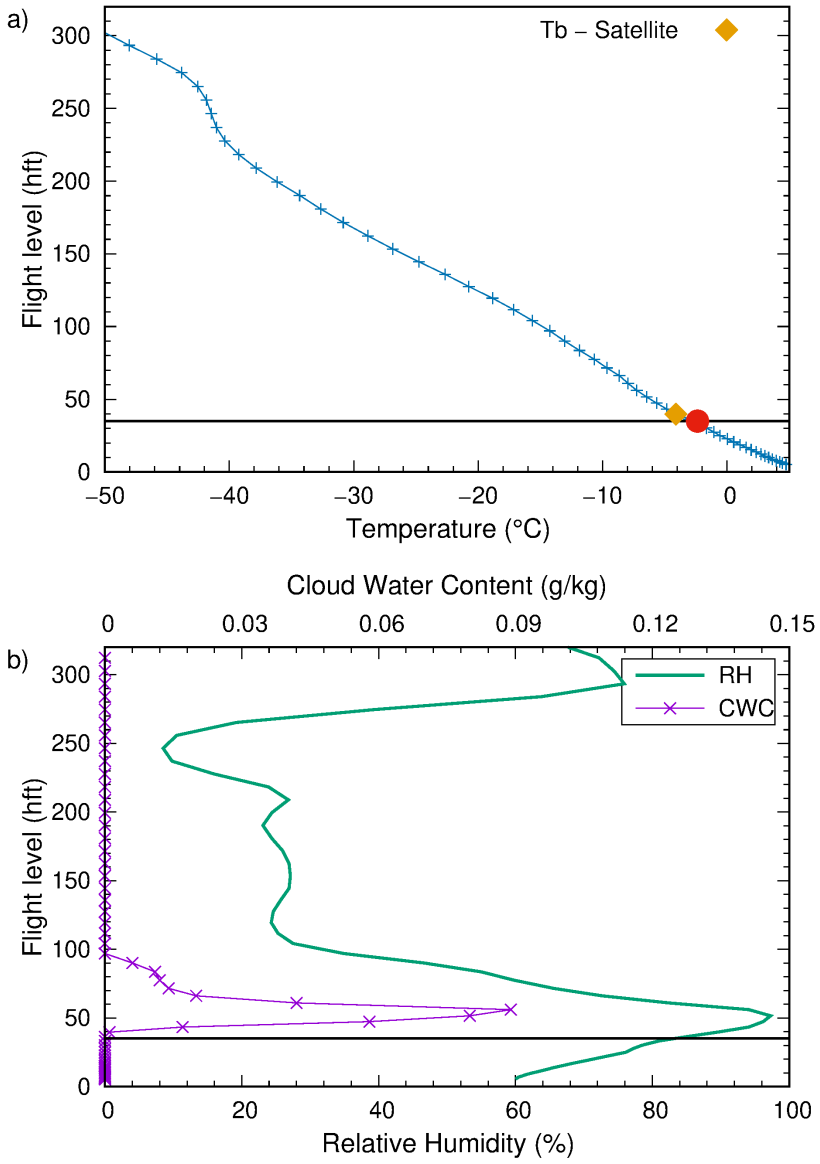

Figure 4.15: Vertical profile of (a) temperature (the red solid circle represents the temperature at the reported altitude) and (b) CWC and RH. The black solid line represents the FL035. The profiles are obtained from the European Centre for Medium-Range Weather Forecasts (H+11) from 1045 UTC on 26 February 2020.

4.2.4 Moderate icing Case - 3 March 2022

Lastly, Figure 4.16 displays the geographical distribution of cloud type, BT10.8 and cloud-top phase at 1230 UTC on 3 March 2020, when a PIREP of moderate icing was issued in mainland Portugal. The region is covered by medium clouds (Figure 4.16 (a)), with a BT10.8 of about $-13°C$ (Figure 4.16 (b)), mostly classified as being composed of ice (Figure 4.16 (c)). To the north of these clouds, low and very low clouds with warmer ($\geq 0°C$) cloud tops are also visible. The latter are characterized by water and mixed-phase cloud tops (Figure 4.16 (c)).

Figure 4.17 shows the vertical profile of temperature, RH and CWC from the ECMWF model at the nearest grid-point with respect to the PIREP location. This figure shows that temperature ranges from $-20°C$ to $0°C$ between FL085 and FL200, where the environment is very favorable to aircraft icing. The reported flight level was FL150, which corresponds to a predicted temperature of $-11°C$. The corresponding flight level of the BT10.8 is approximately FL158. Thus, this icing event occurred near the cloud top. The vertical profile of CWC shows the presence of two cloud layers (using a threshold of $0.01g/kg$): one thin cloud near FL200 and other lower cloud layer between FL70 and FL140. The RH profile suggests the presence of one cloud layer between FL10 and FL140, using a threshold of 80% (lower than in previous cases). At the level of the icing PIREP (FL150), the model predicted a CWC of $0.004g/kg$ and a RH of 74.8%. Thus, the model underestimated the cloud top height, by nearly $20hft$. It is also interesting to note that for this event of moderate icing the values of CWC and RH were lower than those obtained in the previous cases (of severe icing), which is coherent with previous studies (Curry et al. [41] and Cober et al. [35]).

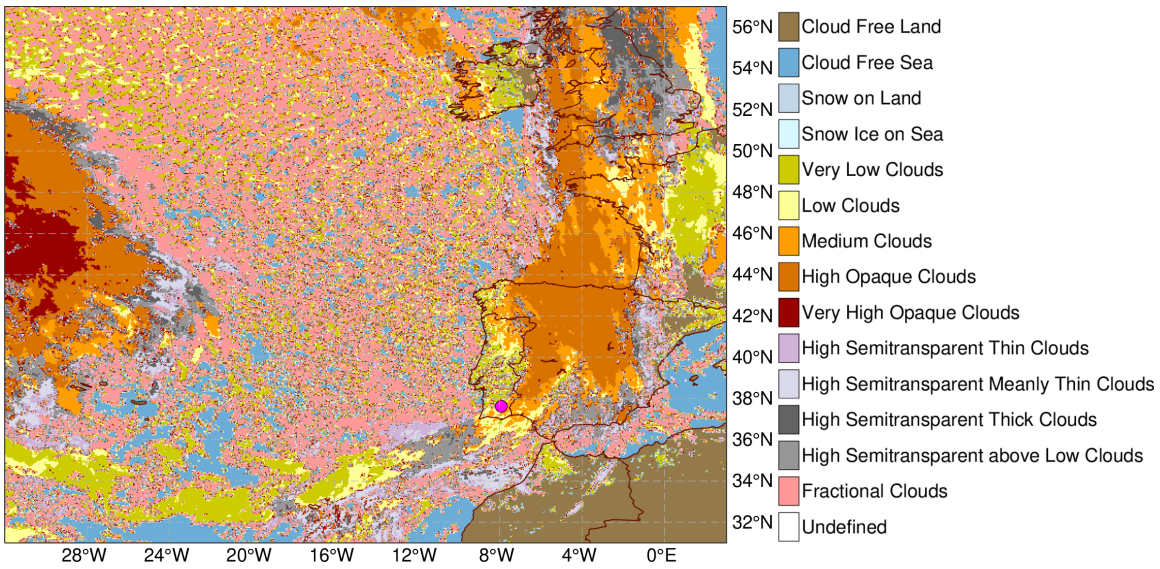

(a) Cloud Type.

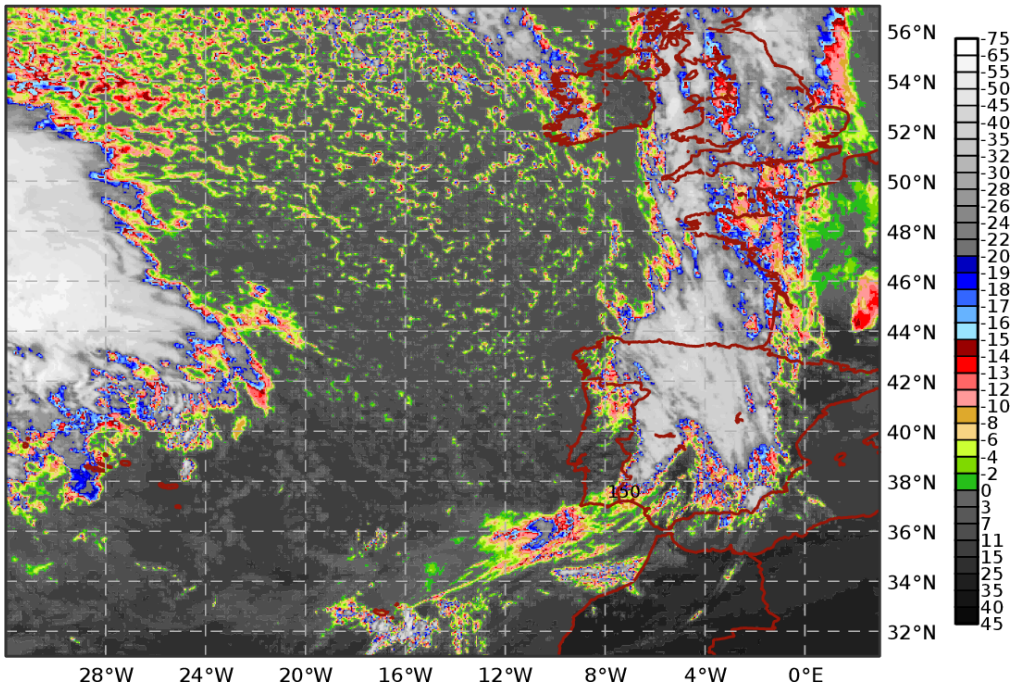

(b) $10.8\mu m$ Brightness Temperature.

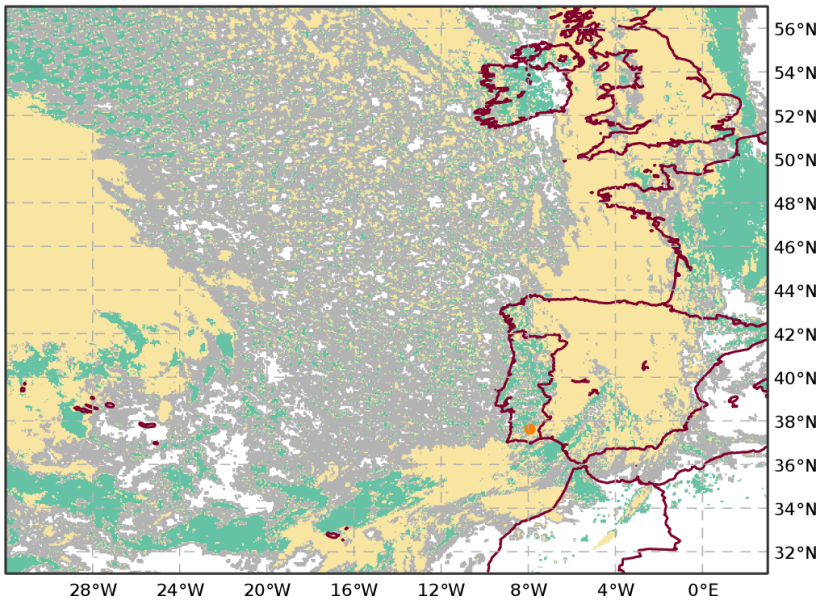

(c) Cloud Phase.

Figure 4.16: Satellite products valid at 1230 UTC on 3 March 2020. The location of the pilot report of moderate icing is represented with a magenta solid circle in the cloud type (a), an orange solid circle cloud phase product (c), and with the FL value in the BT10.8 product (b). The white areas correspond to cloud free areas in the cloud-top phase product (c).

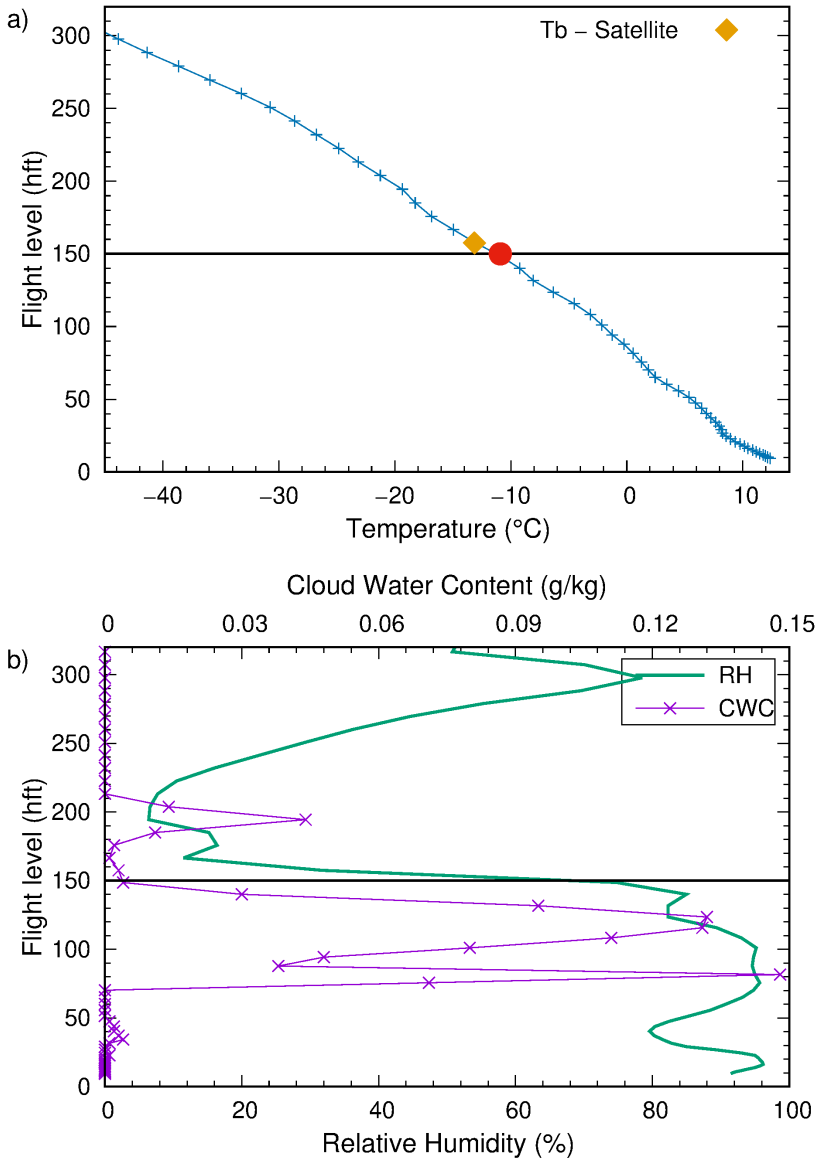

Figure 4.17: Vertical profile of (a) temperature (the red solid circle represents the temperature at the reported altitude) and (b) CWC and RH. The black solid line represents the FL150. The profiles are obtained from the European Centre for Medium-Range Weather Forecasts (H+12) from 1230 UTC on 3 March 2022.

Chapter 5

Conclusions and Future Research

The current study aims to characterize the environment favorable for aircraft icing the in Western Europe and Northeastern Atlantic sector, using PIREPs, satellite data and forecasts from the ECMWF deterministic model. The studied sample comprises 115 icing events, 86 reports of moderate icing and 29 of severe icing, in the region extending from $31°$ to $57°N$ and $3°E$ to $32°W$. Each report contained information on severity, date, time, latitude, longitude and flight level. Satellite products including brightness temperature for the channel centred at $10.8\mu m$, cloud mask, cloud type and cloud-top phase were employed.

Most of the aircraft icing events occurred north to the $45°N$ (72 cases) and during the end of autumn and wintertime ($\approx 70\%$). Besides, 43 cases happened south of $45°N$, mainly in the vicinity of airdromes, with a higher prevalence in December and October. The prevalence of aircraft icing during autumn and winter months is coherent with the higher frequency of frontal systems and relatively cold temperatures during these months. Nevertheless, icing events were also reported during the spring and summer months, in agreement with Sand et al. [33], who also found summer icing encounters. Regarding altitude, most events occurred between FL100 and FL250, with a relative frequency of 82.7% and 78.6%, respectively, for moderate and severe icing events. In contrast, below FL100, the frequency of occurrence is 7% and 18%, respectively, for moderate and severe icing. Above FL250, the frequency of icing events is 10% and 3.5%, respectively, for moderate and severe icing. It should be noted that north of $45°N$ there were more icing events between FL100 and FL150 (20.6%) than above FL250 (2.9%), while south of $45°N$ there were more icing events above FL250 (16.7%) than between FL100 and FL150 (11.9%), which is coherent with higher temperatures at equatorward latitudes.

The preliminary analysis of the cloud mask product showed that nearly 1.2% and 3.5% of the events reported as moderate and severe icing, respectively, were associated with a cloud mask of clear sky. The PIREPs errors in time and location attribution can explain this. Therefore, the PIREPs coordinates were slightly modified, so that the cloud mask of the corrected coordinates would be either partially cloudy or cloud filled. The lowest location error was $5km$ and the highest location error was $58km$.

The analysis of the cloud mask product revealed that the vast majority (96.6%) of severe icing events occurred in a cloud-filled environment, whereas the remaining happened in partially cloudy conditions.

The percentage of cloud-filled cases is slightly lower (88.4%) for moderate icing. Moreover, most of the icing events occurred in medium and high opaque clouds, with BT10.8 between $-40°C$ and $-8°C$ ($\approx 70\%$). On the other hand, nearly 19% of moderate icing and 10% of severe icing were associated with BT10.8 between -56 and $-40°C$, which is not propitious for icing formation. Furthermore, a small percentage of aircraft icing events was associated with high semitransparent clouds. This may reflect the presence of thin cirrus layers overlying medium clouds, where icing may have formed. Finally, nearly 12% of the severe icing events were associated with low clouds and BT10.8 ranging from -4 to $0°C$. Concerning the cloud-top phase product, 60% of the moderate icing events corresponded to a cloud phase of ice, followed by 30.2% and 11.6% with mixed and water. For severe icing, the cases of ice and mixed cloud-top phases had a similar prevalence, approximately 38% and 41%, respectively. As expected, the clouds with tops composed of liquid water droplets were related to higher BT10.8 (minimum of $-34°C$) than clouds tops composed of ice particles (minimum of $-64°C$).

To better illustrate the favorable environment for icing formation in different situations, four case studies were presented: three cases of severe icing and one of moderate icing. For these cases, the forecast profiles of the ECMWF model were examined. The combination of BT10.8 and model data suggest that the first case was associated with a high-level cloud (FL200-FL284) and although the model was able to predict a cloud layer (with RH $\approx 92\%$ and CWC $\approx 0.06 g/kg$) intersecting the PIREP level, apparently it overestimates the cloud-top altitude. In the second case, the model predicts a thick nearly saturated subfreezing layer above FL080 and results suggest that the icing event happened within a thick cloud at nearly $-13°C$ underneath the cloud top (at nearly $-26°C$). The third severe icing event was associated with low clouds with a BT10.8 of $-4°C$ and the presence of liquid water droplets at the top. The last case was a moderate icing event that took place near the top of a cloud with a subfreezing layer from approximately FL080 to FL160, where the BT10.8 was $\approx -13°C$. In this case, the cloud-top phase was ice. In general, the ECMWF model was capable to predict the cloud layers associated to the aircraft icing events, although with errors on the order of $20 hft$ (and $100 hft$ in one case). In addition, the maximum predicted CWC and RH values were $0.18 g/kg$ and 100%, respectively, in a case of severe icing. Also, the four case studies analyzed were associated with high values of RH: $> 74.8\%$.

As discussed early, PIREPs may contain errors in time and location. Moreover, in Europe only moderate and severe icing events are mandatory to report [11] and consequently PIREPs do not provide information about the absence of icing. Therefore, PIREPs are inappropriate to compute standard measures of over forecasting, such as the false-alarm (number of events that were forecast but were not observed) ratio [65]. For these reasons, it is important to use other sources of information to validate or calibrate icing algorithms. The satellite products used in this study can only observe the highest level of clouds and therefore cannot detect icing conditions beneath the cloud top. Nevertheless, these satellite products can provide useful information on the non-icing events, because they can identify the cloud-free areas and areas where subfreezing clouds are absent. In addition, matching satellite data with icing PIREPs can be used to correct the location errors of PIREPs. Then, these validated PIREPs together with information of non-icing events provided by satellite products become very useful for the validation and calibration of icing algorithms, such as that currently used operationally at the Portuguese MWO [9].

This will be the subject of future work. Lastly, other satellite products could also be considered, such as cloud optical thickness and effective droplet radius, so the icing potential could be derived from satellite data [66].

Bibliography

[1] B. A. Hall. Developments in aviation forecasting in the UK. *Meteorological applications*, 5(3):191–204, Dec. 2006.

[2] Z. Pu and E. Kalnay. Numerical Weather Prediction Basics: Models, Numerical Methods, and Data Assimilation. Apr. 2018. In: Duan, Q., Pappenberger, F., Thielen, J., Wood, A., Cloke, H., Schaake, J. (eds) Handbook of Hydrometeorological Ensemble Forecasting. Springer, Berlin, Heidelberg.

[3] J. Mazon, J. I. Rojas, M. Lozano, D. Pino, X. Prats, and M. M. Miglietta. Influence of meteorological phenomena on worldwide aircraft accidents, 1967 - 2010. *Meteorological applications*, 25(2):236–246, Dec. 2017.

[4] G. Vidaurre and J. Hallett. Ice and water content of stratiform mixed-phase cloud. *Quarterly Journal of the Royal Meteorological Society*, 135(642):1292–1306, July 2009.

[5] *Aviation safety, preliminary information on aircraft icing and winter operations, Testimony before the Subcommittee on Aviation, Committee on Transportation and Infrastructure House of Representatives*, 2010. United States Government Accountability Office (GAO).

[6] *Safety Advisor – Aircraft Icing*, 2008. Air Safety Foundation AOPA.

[7] M. Bragg, T. Hutchison, J. Merret, R. Oltman, and D. Pokhariyal. Effect of Ice Accretion on Aircraft Flight Dynamics. 2000. Paper presented at 38th Aerospace Sciences Meeting and Exhibit 2000, Reno, NV, United States.

[8] A. Tafferner, T. Hauf, C. Leifeld, T. Hafner, H. Leykauf, and U. Voigt. ADWICE: Advanced Diagnosis and Warning System for Aircraft Icing Environments. *American Meteorology Society Journals*, 18(2):184–203, Apr. 2003.

[9] M. Belo-Pereira. Comparison of in-flight aircraft icing algorithms based on ECMWF forecasts. *Meteorological Applications*, 22(24):705–715, July 2015.

[10] IPMA. https://www.ipma.pt/en/enciclopedia/aeronautica/index.html. Accessed: 26/09/2022.

[11] *Annex 3 to the Convention on International Civil Aviation. In Meteorological Service for International Air Navigation*, 20^{th} edn., page 224, Montreal, Canada, 2018. International Civil Aviation Organization (ICAO).

[12] B. C. Bernstein, T. A. Omeron, F. McDonough, and M. K. Politovich. The Relationship between Aircraft Icing and Synoptic-Scale Weather Conditions. *Weather and Forecasting*, 12(4):742–762, Dec. 1997.

[13] B. C. Bernstein, R. M. Rasmussen, F. McDonough, and C. Wolff. Keys to Differentiating between Small- and Large-Drop Icing Conditions in Continental Clouds. *Journal of Applied Meteorology and Climatology*, 58(9):1931–1953, Sept. 2019.

[14] G. Thompson, R. T. Bruintjes, B. G. Brown, and F. Hage. Intercomparison of In-Flight Icing Algorithms. Part I: WISP94 Real-Time Icing Prediction and Evaluation Program. *Weather and Forecasting*, 12(4):878–889, July 1997.

[15] M. K. Politovich and T. A. O. Bernstein. Aircraft Icing Conditions in Northeast Colorado. *Journal of Applied Meteorology*, 41(2):118–132, Feb. 2002.

[16] R. M. Rasmussen and Coauthors. Winter Icing and Storms Project (WISP). *Bulletin of the American Meteorological Society*, 73(7):951–974, July 1992.

[17] P. Schultz and M. K. Politovich. Toward the Improvement of Aircraft-Icing Forecasts for the Continental United States. *Weather and Forecasting*, 7(3):491–500, Sept. 1992.

[18] S. Fernández-González, J. L. Sánchez, E. Gascón, L. López, E. García-Ortega, and A. Merino. Weather features associated with aircraft icing conditions: a case study. *Scientific World Journal*, 2014, Feb. 2014.

[19] B. Casqueiro, I. Trigo, and M. Belo-Pereira. Characterization of Icing Conditions using Aircraft Reports and Satellite Data. 2022. Submitted to Atmospheric Research.

[20] A. J. Heymsfield and L. M. Miloshevich. Homogeneous Ice Nucleation and Supercooled Liquid Water in Orographic Wave Clouds. *Journal of Atmospheric Sciences*, 50(15):2335–2353, Aug. 1993.

[21] J. Y. Harrington and P. Q. Olsson. On the potential influence of ice nuclei on surface-forced marine stratocumulus cloud dynamics. *Journal of Geophysical Research*, 106(D21):27473–27484, Nov. 2001.

[22] A. V. Korolev, G. M. Mcfarquhar, P. R. Field, C. N. Franklin, P. Lawson, Z. Wang, E. Williams, S. J. Abel, D. Axisa, S. Borrmann, J. Crosier, J. Fugal, M. Krämer, U. Lohmann, O. Schlenczek, and M. Wendisch. Mixed-Phase Clouds: Progress and Challenges. *Meteorological Monographs*, 58(1): 5.1–5.50, June 2017.

[23] C. D. Ahrens and R. Henson. *Meteorology Today: An Introduction to Weather Climate and the Environment*, chapter 7, pages 179–190. Cengage Learning, 2018.

[24] G. A. Isaac and R. S. Schemenauer. Large Particles in Supercooled Regions of Northern Canadian Cumulus Clouds. *Journal of Applied Meteorology and Climatology*, 18(8):1056–1065, Aug. 1979.

[25] S. G. Cober, J. W. Strap, and G. A. Isaac. An Example of Supercooled Drizzle Drops Formed through a Collision-Coalescence Process. *Journal of Applied Meteorology and Climatology*, 35(12): 2250–2260, Dec. 1996.

[26] D. Rosenfeld and W. L. Woodley. Deep convective clouds with sustained supercooled liquid water down to -37.5°C. *Nature*, 405(6785):440–442, May 2000.

[27] M. Politovich and M. Belo-Pereira. Aircraft icing. *Reference Module in Earth Systems and Environmental Sciences, Elsevier*, Nov. 2015.

[28] *Getting to grips with cold weather operations*, pages 27–37, France, 2000. Airbus Industrie.

[29] B. of Meteorology Aviation Weather Services. Hazardous Weather Phenomena - Airframe Icing, 2015.

[30] Y. Cao, W. Tan, and Z. Wu. Aircraft icing: An ongoing threat to aviation safety. *Aerospace Science and Technology, Elsevier*, 75:353–385, Jan. 2018.

[31] *Aviation Hazards. Education and Training Program ETR-20*, June 2007. WMO/TD-No 1390.

[32] M. Kelsch and L. S. Wharton. Comparing PIREPs with NAWAU Turbulence and Icing Forecasts: Issues and Results. *Weather and Forecasting*, 11(3):385–390, Sept. 1996.

[33] W. Sand, W. Cooper, M. Politovich, and D. Veal. Icing conditions encountered by a research aircraft. *Journal of Climate Applied Meteorology*, 23(10):1427–1440, 1984.

[34] K. Mikkelsen, R. Mcknight, R. Ranaudo, and P. Perkins. Icing flight research - Aerodynamic effects of ice and ice shape documentation with stereo photography. AIAA paper 85-0468, Jan. 1985.

[35] S. G. Cober, G. A. Isaac, and J. W. Strapp. Characterizations of aircraft icing environments that include supercooled large drops. *Journal of Applied Meteorology*, 40(11):1984–2002, 2001.

[36] F.A. Regulations, Part 25-Airworthiness Standards: Transport Category Airplanes, Federal Aviation Administration (FAA), USA, 2013.

[37] M. K. Politovich. Response of a Research Aircraft to Icing and Evaluation of Severity Indices. *Journal of Aircraft*, 33(2):291–297, Mar. 1996.

[38] P. Francis. Detection of aircraft icing conditions over Europe using SEVIRI data. 2007. EUMETSAT Meteorological Satellite Conference/15th AMS Satellite Meteorology and Oceanography Conference, Amsterdam, Netherlands.

[39] G. P. Ellrod and A. A. Bailey. Assessment of Aircraft Icing Potential and Maximum Icing Altitude from Geostationary Meteorological Satellite Data. *Weather and Forecasting*, 22(1):160–174, June 2006.

[40] A. Heinrich, R. Ross, G. Zumwalt, J. Provorse, V. Padmanabhan, J. Thompson, and J. Riley. Aircraft Icing Handbook, Volume 1 of 3. Technical report, FAA Technical Center, Mar. 1991.

[41] J. Curry and G. Liu. Assessment of Aircraft Icing Potential Using Satellite Data. *Journal of Applied Meteorology*, 31(6):605–621, June 1992.

[42] J. Marwitz, M. Politovich, B. Bernstein, F. Ralph, P. Neiman, R. Ashenden, and J. Bresch. Meteorological Conditions Associated with the ATR72 Aircraft Accident near Roselawn, Indiana, on 31 October 1994. *Bulletin of the American Meteorological Society*, 78(1):41–52, Jan. 1997.

[43] B. M. Pobanz, J. D. Marwitz, and M. K. Politovich. Conditions Associated with Large-Drop Regions. *Journal of Applied Meteorology*, 33(11):1366–1372, 1994.

[44] M. K. Politovich. Aircraft Icing Caused by Large Supercooled Droplets. *Journal of Applied Meteorology and Climatology*, 28(9):856–868, Sept. 1989.

[45] C. D. Ahrens. *Meteorology Today: An Introduction to Weather Climate and the Environment*, chapter 5, pages 123–138. 2009. Ninth Edition. Brooks/Cole, Belmont, USA, pp621.

[46] T. Vukits. Overview and risk assessment of icing for transport category aircraft and components. In: 40th AIAA Aerospace Sciences Meeting Exhibit, January 2002, p. 811.

[47] E. Kreeger. Overview of Icing Research at NASA Glenn, Feb. 2013. NASA Glenn Research Center Icing Branch.

[48] R. K. Jeck. A History and Interpretation of Aircraft Icing Intensity Definitions and FAA Rules for Operating in Icing Conditions. Technical report, FAA Technical Center, Nov. 2001.

[49] B. Schwartz. The Quantitative Use of PIREPs in Developing Aviation Weather Guidance Products. *Weather and Forecasting*, 11(3):372–384, Sept. 1996.

[50] J.-M. Carrière, S. Alquier, C. L. Bot, and E. Moulin. Statistical verification of forecast icing risk indices. *Meteorological Applications*, 4(2):115–130, June 1997.

[51] ICAO/METG/DMG. EUR OPMET Data Management Handbook. Technical report, ICAO, Dec. 2021.

[52] B. J.Finlayson-Pitts and J. N. P. Jr. *Chemistry of the Upper and Lower Atmosphere*, chapter 2, pages 15–42. 2000.

[53] C. D. Ahrens. *Meteorology Today: An Introduction to Weather Climate and the Environment*. 1994. Fifth Edition. West Publishing Company, USA, pp592.

[54] EUMETSAT. Meteosat series. https://www.eumetsat.int/our-satellites/meteosat-series. Accessed: 17/08/2022.

[55] J. Schmetz, P. Pili, S. Tjemkes, D. Just, J. Kerkmann, S. Rota, and A. Ratier. An introduction to Meteosat Second Generation (MSG). *Bulletin of the American Meteorological Society*, 83(7): 977–992, July 2002.

[56] C. L. Bot. SIGMA : System of Icing Geographic identification in Meteorology for Aviation. Conference faa in-flight icing - ground de-icing international conference exhibition, Météo France, DPrévi/Aéro, June 2003.

[57] G. Kerdraon and E. Fontaine. *Algorithm Theoretical Basis Document for the Cloud Product Processors of the NWC/GEO*. EUMETSAT, Météo-France - Centre d'études en Météorologie Satellitaire, Oct. 2021.

[58] R. G. Owens and T. D. Hewson. ECMWF Forecast User Guide, 2018. Reading: ECMWF.

[59] S. Malardel, N. Wedi, W. Deconinck, M. Diamantakis, C. Kühnlein, G. Mozdzynski, M. Hamrud, and P. K. Smolarkiewicz. A new grid for the IFS. *ECMWF Newsletter*, 146:23–28, Jan. 2016.

[60] N. H. Center, N. O. Central Pacific Hurricane Center, and A. Administration. https://www.nhc.noaa.gov/gccalc.shtml. Accessed: 23/10/2022.

[61] O. Bruno, C. Hoose, T. Storelvmo, Q. Coopman, and M. Stengel. Exploring the Cloud Top Phase Partitioning in Different Cloud Types Using Active and Passive Satellite Sensors. *Geophysical Research Letters*, 48(2), 2020.

[62] E. Castro, T. Ishida, Y. Takahashi, H. Kubota, G. J. Perez, and J. S. M. Jr. Determination of Cloud-top Height through Three-dimensional Cloud Reconstruction using DIWATA-1 Data. *Scientific Reports*, 10(1)(7570), 2020.

[63] Y. Hu, S. Rodier, K. man Xu, W. Sun, J. Huang, B. Lin, P. Zhai, and D. Josset. Occurrence, liquid water content, and fraction of supercooled water clouds from combined CALIOP/IIR/MODIS measurements. *Journal of Geophysical Research*, 115(D00H34), 2010.

[64] T. Kane, B. Brown, and R. Bruintjes. Characteristics of pilotreports of icing. Preprints. 14^{th} Conference on Probability and Statistics, 11–16 January 1998, Phoenix, AZ.

[65] W. L. S. JR., P. Minnis, C. Fleeger, D. Spangenberg, R. Palikonda, and L. Nguyen. Determining the Flight Icing Threat to Aircraft with Single-Layer Cloud Parameters Derived from Operational Satellite Data. *Journal of Applied Meteorology and Climatology*, 51(10):1794–1810, Oct. 2012.

[66] R. L. Bowyer and P. G. Gill. Objective verification of global in-flight icing forecasts using satellite observations: Verification of WAFS icing forecasts using satellite observations. *Meteorological Applications*, 26(4):610–619, Apr. 2019.

Appendix A

Supporting Figures

The ECMWF temperature profile for the moderate icing event with a positive BT10.8 ($1.4°C$) is depicted in Figure A.1.

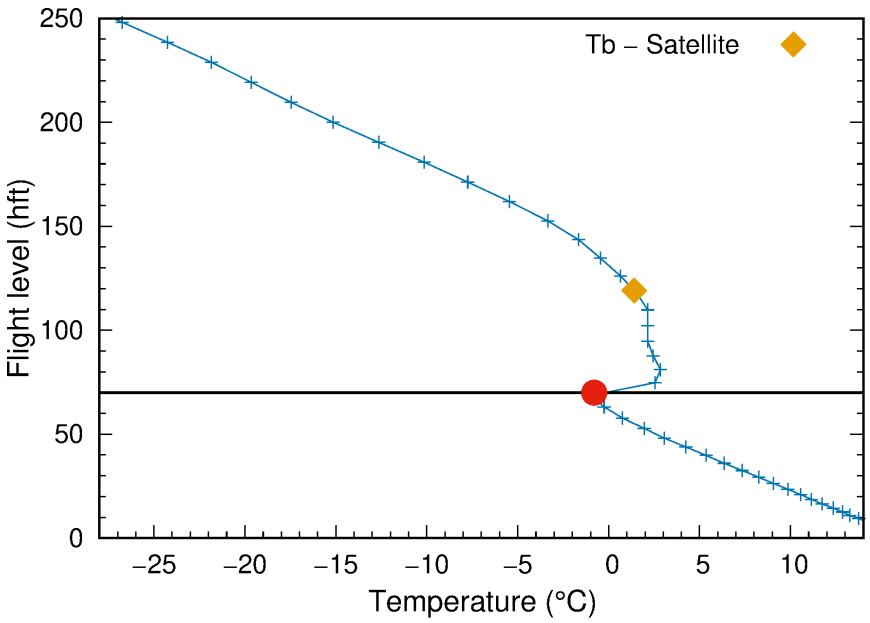

Figure A.1: Vertical profile of temperature (the red solid circle represents the temperature at the reported altitude). The black solid line represents the FL070. The profiles are obtained from the European Centre for Medium-Range Weather Forecasts from 2345 UTC on 22 May 2021.

Figure A.2 shows the distribution of the different values of BT10.8, for the aircraft icing events, for the original data.

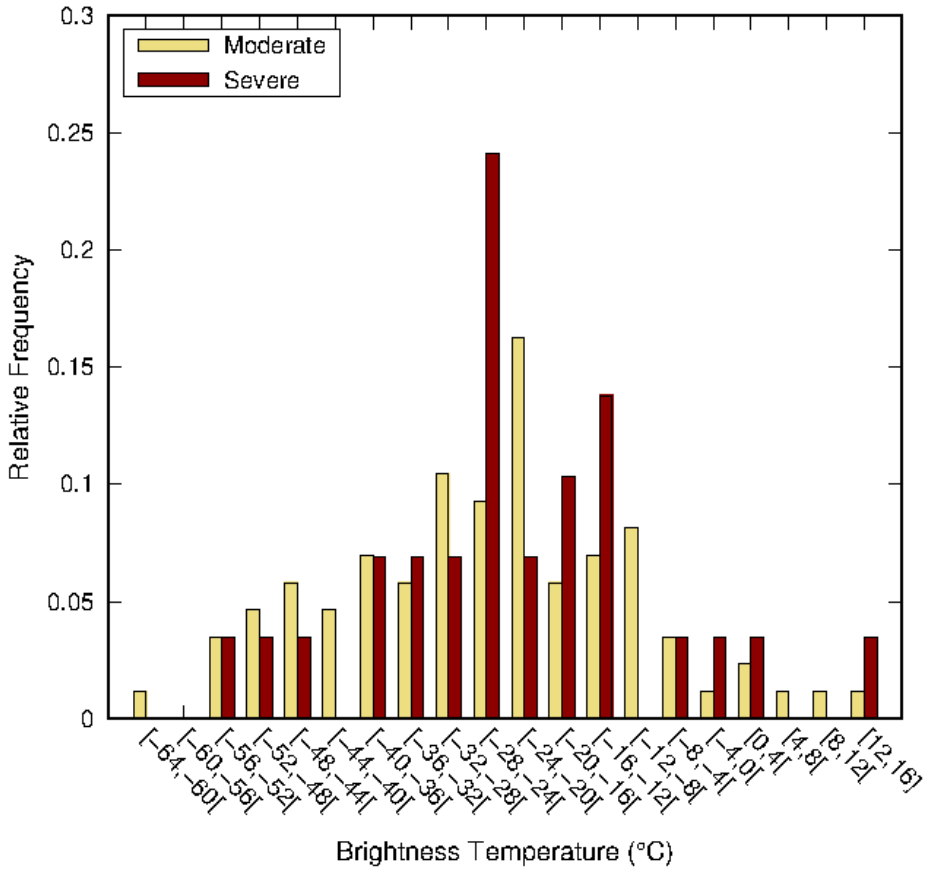

Figure A.2: Relative frequency of different values of BT10.8, for the aircraft icing events, for the original data.